Eur. Phys. J. A **23**, 453–471 (2005)
DOI 10.1140/epja/i2004-10099-3

THE EUROPEAN PHYSICAL JOURNAL A

Subthreshold ϕ-meson production and medium effects in proton-nucleus reactions

E.Ya. Paryev[a]

Institute for Nuclear Research, Russian Academy of Sciences, Moscow 117312, Russia

Received: 4 May 2004 / Revised version: 3 November 2004 /
Published online: 5 January 2005 –
Communicated by A. Molinari

Abstract. Within the spectral function approach we study the direct production and decay via the dikaon (dimuon) channel of ϕ-mesons in the interactions of 2.4 and 2.7 GeV protons with light and medium target nuclei. It is shown that the K^+K^- ($\mu^+\mu^-$) invariant-mass distribution consists of the two components which correspond to the ϕ decay "outside" and "inside" the target nucleus. The first (narrow) component has the free ϕ width, while the second (broad) component is distorted by the nuclear matter due to resonance-nucleon scattering and a possible in-medium modification of the kaons and ρ-meson at finite baryon density. The relative strength of the "inside" and "outside" components is analyzed in different scenarios for the ϕ width and momentum cut. It is demonstrated that the width of the resulting dimuon invariant-mass distribution on medium nuclei is larger than the free ϕ width by a factor of about two if the total ϕ in-medium width is used and the respective cutoff for the ϕ three-momentum is applied, whereas the resulting dikaon invariant-mass distribution has an insignificant sensitivity to the ϕ in-medium properties due to the strong absorption of the K^- in the surrounding nuclear matter. On the other hand, because of the distortion of the K^+ and K^- on their way out the target nucleus mainly due to the hadronic kaon potentials, the latter distribution is broadened and shifted to higher invariant masses, which means that the measurement of such broadening would give additional evidence for the modification of the kaon and antikaon properties in the nuclear medium.

PACS. 25.40.-h Nucleon-induced reactions

1 Introduction

The study of the in-medium properties (like effective masses and widths) of light vector mesons ρ, ω, ϕ through their production and decay in nucleus-nucleus and proton-nucleus collisions as well as in pion- and photon-induced reactions has received considerable interest in recent years (see, for example, refs. [1–61]) and is one of the most exciting topics of the nuclear and hadronic physics nowadays. This interest was triggered by the universal scaling hypothesis of Brown and Rho [62] as well as a QCD-sum-rule–based prediction of Hatsuda and Lee [63] that the masses of these mesons should drop in nuclear matter due to a partial restoration of chiral symmetry, which is characterized by a reduction of the order parameter of spontaneously broken chiral symmetry —the scalar quark condensate $\langle\bar{q}q\rangle$— in the medium compared to its vacuum magnitude. The evolution of this order parameter with increasing temperature and/or density and the possible restoration of chiral symmetry above some critical temperature and density (the chiral phase transition) accompanied, as is expected [27,64,65], by the phase transition from composite hadrons to a Quark-Gluon Plasma (the deconfinement transition) are the key issues [27,64–66] which motivate the field of heavy-ion collisions and reactions of elementary probes with nuclei at high initial energies.

On the other hand, as has been emphasized in the literature [27,59,67–71], the properties of hadrons embedded into the nuclear matter are modified due to their standard many-body interactions with the surrounding nucleons. In the conventional hadronic models, based on effective hadronic Lagrangians, the in-medium properties of the light vector mesons, *i.e.* in the general case their in-medium self-energies (or in-medium spectral functions) are calculated by dressing their propagators with the appropriate hadronic loops [72–76] or, using the low-density approximation, they are expressed via the free forward meson-nucleon scattering amplitudes [77–80]. As a result, the relationship between the observed modifications of the properties of these mesons in matter and chiral symmetry restoration is not evident [27,81].

In this respect the ϕ-meson stands as a unique probe for a possible restoration of chiral symmetry in the strange

[a] e-mail: paryev@inr.ru

sector, since due to the weakness of the conventional ϕN interaction its possible mass shift in nuclear matter, as is expected [44] basing on the QCD sum rule approaches [63, 82], is related mostly to the in-medium strange-quark condensate $\langle \bar{s}s \rangle$ behavior. This behavior for not too high densities and temperatures is almost entirely governed by the strangeness content of the nucleon [44,63] —the quantity which is poorly known so far and is currently of great interest [83–86]. Thus, the measurement of the in-medium phi-meson mass is expected to provide an information about the nucleon strangeness content [39]. In addition to the above exotic prospects, the ϕ-meson is of further interest because of the following reasons. Firstly, the enhanced production of ϕ-mesons in relativistic nucleus-nucleus collisions could be one of the signatures of the creation of the Quark-Gluon Plasma (QGP) phase in these collisions [87, 88], since in the environment of a QGP the copious s and $\bar{s}$ quarks originating from gluon annihilation would be very likely to coalesce forming ϕ-mesons during the hadronization phase, while the production of ϕ in hadron-hadron interactions is suppressed due to the OZI rule [88]. Secondly, since the phi mesons interact weakly with non-strange hadrons, they will keep information about the early stage of the colliding system and the reaction dynamics. Thirdly, the ϕ-meson (in contrast to the ρ and ω mesons) does not overlap with other light resonances in the mass spectrum. Finally, the small decay energy for the channel $\phi \to K^+K^-$ and the narrow total width ($\Gamma_\phi = 4.45$ MeV) make this decay mode very sensitive to the medium modification of both kaon and ϕ [38–40,89].

The ϕ mass and width modifications in matter have been studied in various approaches based both on the QCD sum rules [63,82,90] and on the hadronic models [73–76,89,91–93]. All these models agree in establishing that in nuclear medium the shift of the ϕ-meson mass is very small (about 1–2% of its free mass at normal nuclear matter density ρ_0), whereas the in-medium decay width of the phi meson increases compared to the vacuum value by about an order of magnitude at ρ_0 such that its lifetime at $\rho = \rho_0$ is reduced to less than 5 fm/c. As a result, ϕ-mesons embedded with small velocity in a nucleus have a good chance to decay within nuclear matter. Experimentally, the ϕ-meson can be detected from both its hadronic ($\phi \to K^+K^-$) and leptonic ($\phi \to e^+e^-$, $\phi \to \mu^+\mu^-$) decay channels. The latter channel, in spite of its weakness ($BR(\phi \to e^+e^-, \phi \to \mu^+\mu^-) \approx 3 \cdot 10^{-4}$), is apparently best suited for the study of the ϕ properties in a hot and dense matter because of the minimal final-state interactions of the daughter leptons, while the reconstruction of a ϕ-meson decay inside a medium via hadronic mode is expected to be hindered by the interactions of daughter kaons with surrounding hadronic environment. The change of these properties would be clearly revealed in the invariant-mass spectra of the dileptons through the shoulder slightly below the ϕ resonant peak and broadening of its spectral function [39].

Phi-meson production in heavy-ion collisions has been studied at various energies. At SIS energies it was measured by the FOPI Collaboration [20,21] in central Ni + Ni collisions through the K^+K^- invariant-mass distribution. A large ϕ production probability and a ϕ/K^- ratio of the order of unity have been observed, which cannot be reproduced with present transport codes [38, 94] taking into account in-medium effects both on the ϕ-meson and on the kaon masses. The production of ϕ-mesons in central Si + Au interactions at 14.6 A GeV/c has also been measured at AGS/BNL by the E802 Collaboration [17] via the dikaon invariant-mass spectrum. The measured phi-meson mass distribution was found to be consistent with that in free space. The ϕ/K^- ratio was, in contrast to the preceding case, about 10%. At SPS energies phi-meson production has been previously measured by the HELIOS-3 Collaboration [10,11] and by the NA38 Collaboration [13] through the dimuon invariant-mass spectra. A factor of 2 to 3 enhancement in the double ratio $(\phi/(\rho+\omega))_{SU(W)}/(\phi/(\rho+\omega))_{pW}$ was observed. This enhancement may be a signature of the formation of a QGP in the collisions [88]. On the other hand, it can also be explained in hadronic models if one takes into consideration the mass shift of the ϕ-meson in nuclear medium [95]. Recently, new experimental data on ϕ-meson production in central Pb + Pb collisions at 158 GeV/nucleon beam energy became available from CERN/SPS. The NA49 Collaboration [96] has identified the ϕ-meson via its hadronic decay $\phi \to K^+K^-$, while the NA50 Collaboration [97] measured it using the leptonic decay $\phi \to \mu^+\mu^-$. It was found that the extracted phi-meson yield from dimuon channel exceeds by a factor of 2–4 that extracted from the dikaon channel (the so-called ϕ-meson puzzle). This difference has been studied in a multiphase transport model [40], which took into account both the rescatterings of the K^+ and K^- in the hadronic matter and in-medium mass modifications of kaons and ϕ-mesons. It was shown that the phi-meson yields reconstructed from dikaon and dimuon channels differ by a factor of two, which corresponds only to the lower bound to the differences found in the NA49 and NA50 data. Finally, the first results on phi mesons from the Relativistic Heavy Ion Collider (RHIC) have started to appear. The STAR Collaboration [98] reported recently the experimental data on the transverse mass spectra of ϕ-mesons produced in Au + Au collisions at the energy $\sqrt{s} = 130$ A GeV. Phi-meson production has also been measured recently in 12 GeV p + C and p + Cu reactions at KEK/PS by the E325 Collaboration [24] through the K^+K^- invariant-mass spectra. Any signature of in-medium modification of the ϕ-meson has not been observed. At the same time, this Collaboration has found [23,24] a statistically significant excess for the copper target in the e^+e^- invariant-mass spectra below the ρ/ω peak over the known physical processes, which indicates that the spectral shape of ρ/ω is modified already at the density of ordinary nuclei. It should be pointed out that the measurements of the elementary processes $pp \to pp\phi$ [99] and $\gamma p \to p\phi$ [100,101] near threshold have been conducted in the recent past.

Besides the above experiments, recently many experimental efforts have also started to shed light on the possible modification of the ϕ-meson in nuclear matter.

The measurements of the leptonic and the hadronic decay modes of the ϕ are planned in the near future at the SIS/GSI accelerator using proton and heavy-ion beams in the HADES detector system [102,103]. Phi-meson production in pp and pA collisions close to threshold is also planned to be studied via the dikaon invariant-mass spectra at the accelerators NUCLOTRON-Dubna [104] and COSY-Jülich [105]. The experiment on photoproduction of ϕ-mesons from nuclei, looking for the A-dependence of the ϕ production cross-sections, will be performed soon at the Spring 8/Osaka facility [106] using a photon beam of 2.4 GeV maximum energy, which is produced by backward Compton scattering of laser photons from 8 GeV electrons.

On the theoretical side, several calculations have been done recently [58,59,107–109] to analyze the feasibility to study the medium modification of the ϕ-meson at the density of ordinary nuclei in the threshold energy region —the main goal of the present investigation. In particular, the authors of ref. [58], applying many-body techniques for evaluating the photon self-energy diagram in nuclear matter which accounts for ϕ-ph production in intermediate states, or analogously the $\gamma N \to \phi N$ reaction inside the nucleus, found that the width of the invariant K^+K^- mass distribution for ϕ photoproduction on medium nuclei is larger than its free width by a factor of about two. On the other hand, the work [59], based on the BUU transport model calculations, points at an insignificant sensitivity of the K^+K^- mass distribution in photonuclear reactions to the ϕ properties at finite baryon density when the Coulomb corrections are included. A BUU-type transport model has also been employed very recently [107] to calculate the target mass dependence of the ϕ total production cross-section reconstructed from the K^+K^- and the e^+e^- decay channels in near-threshold proton-nucleus collisions. It was found that a strong K^- potential leads to a measurable change of the behavior of this cross-section as a function of the target mass. The authors of [108, 109] using present models for the ϕ self-energy in a nuclear medium and an eikonal approximation to account for the distortion of the outgoing ϕ-meson have shown that the A-dependence of the relative cross-sections for ϕ production in nuclei in photon- and proton-induced reactions bears valuable information on the ϕ width in the nuclear medium.

In this paper we perform a detailed study of the production and decay via the dikaon and dimuon channels of ϕ-mesons in pA reactions at 2.4 and 2.7 GeV beam energies. Some preliminary results of this study have been reported in ref. [110]. We present the detailed predictions for the double differential invariant-mass spectra of the K^+K^- and $\mu^+\mu^-$ pairs originating from ϕ-meson decays inside and outside the target nucleus in $p + {}^{12}$C and $p + {}^{63}$Cu reactions obtained in the framework of a nuclear spectral function approach [111–115] for an incoherent primary proton-nucleon ϕ-meson production process. We investigate the effect of in-medium ϕ-meson broadening due to its two-body collisions with nucleons in the nuclear environment and a possible kaon and rho-meson mass shifts in that environment on these spectra. In addition we evaluate the influence of the distortion of the K^+ and K^- on their way out the target nucleus due to the Coulomb and the hadronic kaon potentials on the K^+K^- mass spectrum.

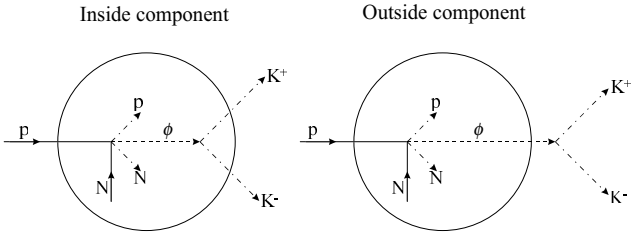

Fig. 1. A contribution to the (p, K^+K^-) reaction on the nuclear target via the production/decay sequence $pN \to pN\phi$, $\phi \to K^+K^-$.

2 Model and results

2.1 The ϕ spectral function

An incident proton can produce a ϕ directly in the first inelastic pN collision due to the nucleon's Fermi motion. Since we are interested in the few-GeV region, we have taken into account the following elementary process[1] which has the lowest free production threshold (2.59 GeV):

$$p + N \to p + N + \phi. \tag{1}$$

Then the produced ϕ-meson can decay into the K^+K^- or $\mu^+\mu^-$ pairs of our interest

$$\phi \to K^+K^-, \tag{2}$$

$$\phi \to \mu^+\mu^-, \tag{3}$$

not only inside a nuclear medium but also outside it. The processes (1), (2) are depicted schematically in fig. 1. As a result, the mass distribution of ϕ resonance decay products is expected to have a two-component structure [116] corresponding to decays outside and inside the nucleus. The first (very narrow) component corresponds to the ϕ-mesons decaying in the vacuum, thus showing the free spectral function. The second (broader) component corresponds to the ϕ decay inside the nucleus. It is evident that most of the ϕ-mesons will decay outside the nucleus due to the small width and the large momentum

[1] For the sake of numerical simplicity, we neglect the production of ϕ-mesons in collisions of secondary pions with intranuclear nucleons. Evidently, this enables us to obtain a lower estimate of the strength of the respective dikaon (dimuon) invariant-mass cross-sections and has basically no influence (cf. [59]) on their shape of our main interest since, due to the rather strong absorption of the final-state antikaons, these cross-sections are simply sensitive to the nuclear surface (see below). Therefore, the production mechanism, if of primary or secondary nature, has basically no influence on the observables apart from the full strength of the calculated cross-sections.

of the ϕ resonance. Therefore, at first sight, the observation of the modification of its properties in the nuclear medium through the dikaon (dimuon) invariant-mass spectrum seems rather unlikely. To avoid this problem the authors of ref. [58] proposed to restrict the three-momenta of the observed K^+K^- pairs (and hence of the produced ϕ-mesons) to about 100–150 MeV/c in order to guarantee that a substantial fraction of events stems from ϕ decays inside the nucleus. This momentum cut will be also applied in the present work.

In our model the ϕ free spectral function is parametrized by a relativistic Breit-Wigner distribution [56,59]

$$S_\phi(m_\phi) = \frac{2}{\pi} \frac{m_\phi^2 \Gamma_{\rm tot}(m_\phi)}{(m_\phi^2 - M_\phi^2)^2 + m_\phi^2 \Gamma_{\rm tot}^2(m_\phi)}, \qquad (4)$$

where m_ϕ is the invariant mass of the ϕ, M_ϕ denotes its pole mass ($M_\phi = 1019.417$ MeV [117]) and $\Gamma_{\rm tot}(m_\phi)$ is the total mass-dependent width in its rest frame ($\Gamma_{\rm tot}(M_\phi) = 4.45$ MeV [117]). The main decay channels of the ϕ-meson, which exhaust almost completely its total width $\Gamma_{\rm tot}$, are $\phi \to K^+K^-$ ($BR(\phi \to K^+K^-) \approx 50\%$), $\phi \to K^0\bar{K}^0$ ($BR(\phi \to K^0\bar{K}^0) \approx 33\%$) and $\phi \to \rho\pi$ ($BR(\phi \to \rho\pi) \approx 17\%$). For the mass dependence of these partial widths we adopt the following parametrizations [56,118–120][2]:

$$\Gamma_{\phi\to K\bar{K}}(m_\phi) = \Gamma_{\phi\to K\bar{K}}(M_\phi) \times \frac{M_\phi}{m_\phi} \frac{\overset{*}{p}_{K\bar{K}}(m_\phi)}{\overset{*}{p}_{K\bar{K}}(M_\phi)} \frac{B_1^2[\overset{*}{p}_{K\bar{K}}(m_\phi)\tilde{R}]}{B_1^2[\overset{*}{p}_{K\bar{K}}(M_\phi)\tilde{R}]}, \qquad (5)$$

$$\Gamma_{\phi\to\rho\pi}(m_\phi) = \Gamma_{\phi\to\rho\pi}(M_\phi) \times \frac{M_\phi}{m_\phi} \frac{\overset{*}{p}_{\rho\pi}(m_\phi)}{\overset{*}{p}_{\rho\pi}(M_\phi)} \frac{B_1^2[\overset{*}{p}_{\rho\pi}(m_\phi)\tilde{R}]}{B_1^2[\overset{*}{p}_{\rho\pi}(M_\phi)\tilde{R}]}, \qquad (6)$$

where $\Gamma_{\phi\to K\bar{K}}(M_\phi)$ and $\Gamma_{\phi\to\rho\pi}(M_\phi)$ are the respective partial decay widths at the pole of the resonance, while $\overset{*}{p}_{K\bar{K}}$, $\overset{*}{p}_{\rho\pi}$ and B_1 are given by

$$\overset{*}{p}_{K\bar{K}}(m_\phi) = \frac{1}{2m_\phi}\lambda(m_\phi^2, m_K^2, m_{\bar{K}}^2),$$
$$\overset{*}{p}_{\rho\pi}(m_\phi) = \frac{1}{2m_\phi}\lambda(m_\phi^2, M_\rho^2, m_\pi^2), \qquad (7)$$

$$\lambda(x,y,z) = \sqrt{[x-(\sqrt{y}+\sqrt{z})^2][x-(\sqrt{y}-\sqrt{z})^2]}; \qquad (8)$$

$$B_1^2(x) = \frac{x^2}{1+x^2}. \qquad (9)$$

Here, $\{K\bar{K}\}$ stands for $\{K^+K^-\}$ or $\{K^0\bar{K}^0\}$; $m_K(m_{\bar{K}})$, M_ρ and m_π are the masses in free space of a kaon (antikaon), ρ-meson and π-meson, respectively, and B_1 is a Blatt-Weisskopf barrier penetration factor (interaction radius $\tilde{R} = 1$ fm). The total decay width $\Gamma_{\rm tot}$, entering into eq. (4), is given by the sum over the partial widths of main ϕ decay channels:

$$\Gamma_{\rm tot}(m_\phi) = \Gamma_{\phi\to K^+K^-}(m_\phi) + \Gamma_{\phi\to K^0\bar{K}^0}(m_\phi) + \Gamma_{\phi\to\rho\pi}(m_\phi). \qquad (10)$$

Following [38–40,52–56,59], we assume that the in-medium ϕ-meson spectral function $S_\phi(\mathbf{r}, m_\phi)$ can also be described by the Breit-Wigner formula (4) with a total width distorted by the possible change of kaon and ρ masses in nuclear environment as well as by ϕN collisions[3]:

$$\Gamma_{\rm tot}(\mathbf{r}, m_\phi) = \Gamma_{\phi\to K^+K^-}(\mathbf{r}, m_\phi) + \Gamma_{\phi\to K^0\bar{K}^0}(\mathbf{r}, m_\phi) + \Gamma_{\phi\to\rho\pi}(\mathbf{r}, m_\phi) + \Gamma_{\rm coll}(\mathbf{r}). \qquad (11)$$

Here, $\Gamma_{\phi\to K\bar{K}}(\mathbf{r}, m_\phi)$ and $\Gamma_{\phi\to\rho\pi}(\mathbf{r}, m_\phi)$ are the partial widths of the $\phi \to K\bar{K}$ and $\phi \to \rho\pi$ decays in nuclear medium at spatial coordinate $\mathbf{r}$, while $\Gamma_{\rm coll}(\mathbf{r})$ denotes the collisional width due to ϕN interactions. Assuming that the $\phi K\bar{K}$ and $\phi\rho\pi$ coupling constants are not modified at the finite baryon density ρ_N of interest, we get for the in-medium widths $\Gamma_{\phi\to K\bar{K}}(\mathbf{r}, m_\phi)$ and $\Gamma_{\phi\to\rho\pi}(\mathbf{r}, m_\phi)$ the expressions analogous to (5) and (6):

$$\Gamma_{\phi\to K\bar{K}}(\mathbf{r}, m_\phi) = \Gamma_{\phi\to K\bar{K}}(\mathbf{r}, M_\phi) \times \frac{M_\phi}{m_\phi} \frac{\overset{*}{p}_{K\bar{K}}(\mathbf{r}, m_\phi)}{\overset{*}{p}_{K\bar{K}}(\mathbf{r}, M_\phi)} \frac{B_1^2[\overset{*}{p}_{K\bar{K}}(\mathbf{r}, m_\phi)\tilde{R}]}{B_1^2[\overset{*}{p}_{K\bar{K}}(\mathbf{r}, M_\phi)\tilde{R}]}, \qquad (12)$$

$$\Gamma_{\phi\to\rho\pi}(\mathbf{r}, m_\phi) = \Gamma_{\phi\to\rho\pi}(\mathbf{r}, M_\phi) \times \frac{M_\phi}{m_\phi} \frac{\overset{*}{p}_{\rho\pi}(\mathbf{r}, m_\phi)}{\overset{*}{p}_{\rho\pi}(\mathbf{r}, M_\phi)} \frac{B_1^2[\overset{*}{p}_{\rho\pi}(\mathbf{r}, m_\phi)\tilde{R}]}{B_1^2[\overset{*}{p}_{\rho\pi}(\mathbf{r}, M_\phi)\tilde{R}]}; \qquad (13)$$

$$\overset{*}{p}_{K\bar{K}}(\mathbf{r}, m_\phi) = \frac{1}{2m_\phi}\lambda(m_\phi^2, m_K^{*2}(\mathbf{r}), m_{\bar{K}}^{*2}(\mathbf{r})),$$
$$\overset{*}{p}_{\rho\pi}(\mathbf{r}, m_\phi) = \frac{1}{2m_\phi}\lambda(m_\phi^2, M_\rho^{*2}(\mathbf{r}), m_\pi^2), \qquad (14)$$

in which the in-medium partial widths $\Gamma_{\phi\to K\bar{K}}(\mathbf{r}, M_\phi)$ and $\Gamma_{\phi\to\rho\pi}(\mathbf{r}, M_\phi)$ at the pole of the resonance are related to the corresponding vacuum widths $\Gamma_{\phi\to K\bar{K}}(M_\phi)$ and $\Gamma_{\phi\to\rho\pi}(M_\phi)$ as follows:

$$\Gamma_{\phi\to K\bar{K}}(\mathbf{r}, M_\phi) = \Gamma_{\phi\to K\bar{K}}(M_\phi) \times \frac{\overset{*}{p}_{K\bar{K}}(\mathbf{r}, M_\phi)}{\overset{*}{p}_{K\bar{K}}(M_\phi)} \frac{B_1^2[\overset{*}{p}_{K\bar{K}}(\mathbf{r}, M_\phi)\tilde{R}]}{B_1^2[\overset{*}{p}_{K\bar{K}}(M_\phi)\tilde{R}]}, \qquad (15)$$

$$\Gamma_{\phi\to\rho\pi}(\mathbf{r}, M_\phi) = \Gamma_{\phi\to\rho\pi}(M_\phi) \times \frac{\overset{*}{p}_{\rho\pi}(\mathbf{r}, M_\phi)}{\overset{*}{p}_{\rho\pi}(M_\phi)} \frac{B_1^2[\overset{*}{p}_{\rho\pi}(\mathbf{r}, M_\phi)\tilde{R}]}{B_1^2[\overset{*}{p}_{\rho\pi}(M_\phi)\tilde{R}]}. \qquad (16)$$

Here, m_K^*, $m_{\bar{K}}^*$ and M_ρ^* are the effective masses, respectively, of kaon, antikaon and ρ-meson in nuclear matter. As

[2] It should be pointed out that expression (6) for the partial width $\Gamma_{\phi\to\rho\pi}(m_\phi)$ has been obtained in the zero-width approximation for the ρ-meson spectral function. This is well justified due to a rather small contribution from the $\rho\pi$-channel into the total ϕ width. For simplicity, we will also ignore below the width of the rho meson in matter, but take into account its pole mass shift.

[3] In using (4) to describe the in-medium ϕ-meson we will neglect [43,58,59] the small downward shift of its pole mass of about 10 MeV [74,76] at saturation density.

in ref. [114], in the following calculations we will employ for the kaon and antikaon in-medium masses the linear extrapolation of the form

$$m^*_{K(\bar{K})}(\mathbf{r}) = m_{K(\bar{K})} + U_{K(\bar{K})}(\rho_N(\mathbf{r})) \tag{17}$$

with[4]

$$U_K(\rho_N) = 22\frac{\rho_N}{\rho_0}\ \text{MeV},\ \ U_{\bar{K}}(\rho_N) = -126\frac{\rho_N}{\rho_0}\ \text{MeV}. \tag{18}$$

An analogous extrapolation can be used as well, as was shown by Hatsuda and Lee [63] basing on a QCD sum rules calculation in zero-width approximation, to model the effective pole mass of a rho meson[5] in the nuclear environment:

$$M^*_\rho(\mathbf{r}) = M_\rho\left(1 - \alpha_\rho\frac{\rho_N(\mathbf{r})}{\rho_0}\right), \tag{19}$$

where $M_\rho = 770$ MeV and $\alpha_\rho = 0.18$. We do not consider the change of a ϕ decay width $\Gamma_{\phi\to\rho\pi}$ in a nuclear medium due to the modification of pion properties. The shift of a pion mass produces a minor effect [43], and it is, therefore, neglected here.

When the slow in the rest frame of the nucleus ϕ-mesons produced are considered, the collisional width $\Gamma_{\rm coll}(\mathbf{r})$ due to ϕN interactions (among which the processes $\phi N \to K\Lambda$, $\phi N \to K\Sigma^*$ are the dominant[6] ones [38–40,75,76,92]) can be represented in the following form [48,49,52–57,59]:

$$\Gamma_{\rm coll}(\mathbf{r}) = \Gamma^0_{\rm coll}\frac{\rho_N(\mathbf{r})}{\rho_0}, \tag{20}$$

where the collisional width $\Gamma^0_{\rm coll}$ at saturation density ρ_0, as follows from [52,75], amounts approximately to 10 MeV.

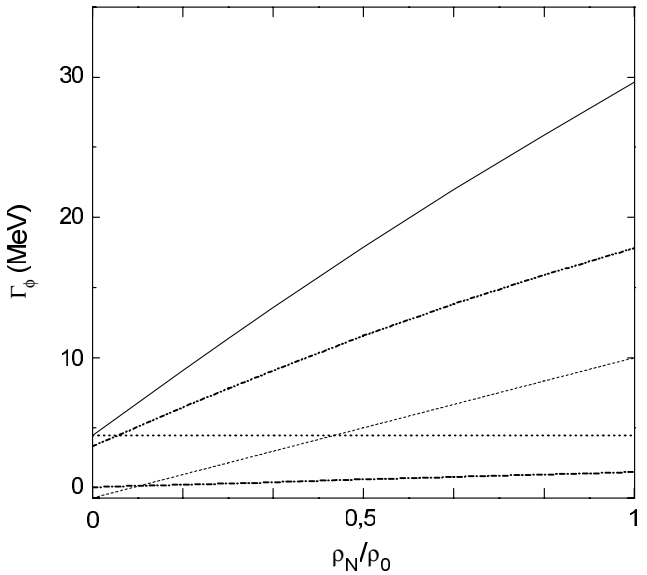

Fig. 2. Phi-meson partial decay widths, collisional width and total width as functions of density. For notation see text.

As for the partial width $\Gamma_{\phi\to\mu^+\mu^-}(m_\phi)$ of the decay channel (3), which will be used in our calculations of the dimuon invariant-mass spectra[7] from pA collisions, it is given by [40]

$$\Gamma_{\phi\to\mu^+\mu^-}(m_\phi) = C_{\mu^+\mu^-}\frac{M^4_\phi}{m^3_\phi} \times\left(1 - \frac{4m^2_\mu}{m^2_\phi}\right)^{1/2}\left(1 + \frac{2m^2_\mu}{m^2_\phi}\right), \tag{21}$$

where m_μ is the rest mass of a muon and the coefficient $C_{\mu^+\mu^-}$ determined from the measured branching ratio for this channel at $m_\phi = M_\phi$ ($2.9\cdot10^{-4}$ [117]) is equal to $1.267\cdot10^{-6}$. As in ref. [40], we will neglect in our subsequent calculations the possible modification of this coefficient in nuclear medium.

In fig. 2 we show the density dependence of the phi partial widths $\Gamma_{\phi\to K\bar{K}}(\mathbf{r}, M_\phi) = \Gamma_{\phi\to K^+K^-}(\mathbf{r}, M_\phi) +$

[4] It should be noted that recent self-consistent approaches based on the chiral Lagrangians [121–125] or meson exchange potentials [126,127] predict also a relatively shallow low-energy antikaon-nucleus potential with a central depth of the order of 40–60 MeV. To see what are the effects of the antikaon optical potential on the observables under consideration we have performed an additional calculation (compared to those presented below in fig. 12) of the $\mu^+\mu^-$ invariant-mass distribution from $p+{}^{63}$Cu reactions at 2.4 GeV incident energy by adopting the $\bar{K}$ potential $U_{\bar{K}}(\rho_N) = -50(\rho_N/\rho_0)$ MeV instead of potential (18). All other parameters (the kaon and ρ-meson mass shifts at saturation density as well as the phi collisional width at the same density and the ϕ momentum cut) employed in the calculation were identical to those used in the calculation denoted by the solid line in fig. 12. As a result, the strength of the total dimuon production cross-section at the peak was increased by a factor of about 1.5 compared to that (see solid line in fig. 12) calculated using a relatively deep antikaon potential of depth 126 MeV. Whereas the width of this cross-section was decreased of 0.3 MeV compared to that (6.4 MeV) found in the latter case.

[5] It is worth noting that the authors of [90,128,129] have pointed out recently that the in-medium QCD sum rules are also satisfied with larger ρ masses if their width is broad enough. Many conventional theoretical approaches (see, for example, refs. [68–71,130–135]) also predict that, as a function of nucleon density, the ρ-meson spectral function is strongly enhanced at low masses, while the maximum, *i.e.*, the pole mass, is slightly shifted upwards. However, due to a rather small contribution from the $\rho\pi$-channel into the total ϕ width, a minor effect on the dikaon (dimuon) yield considered below is expected if one employs this in-medium–modification scheme of the ρ-meson instead of a dropping ρ mass scenario (19).

[6] It should be noted that the contribution of the reaction $\phi N \to K\Sigma$ to the collisional width $\Gamma_{\rm coll}(\mathbf{r})$ is found [38,75,76] to be quite small compared to that from the processes $\phi N \to K\Lambda$ and $\phi N \to K\Sigma^*$. This is mainly due to the fact that the $\bar{K}N\Sigma$ coupling constant is much smaller than those of $\bar{K}N\Lambda$ and $\bar{K}N\Sigma^*$ [38,75,76].

[7] Since $\Gamma_{\phi\to\mu^+\mu^-}(m_\phi) \approx \Gamma_{\phi\to e^+e^-}(m_\phi)$ [56], these spectra can also be treated as the respective dielectron ones.

$\Gamma_{\phi\to K^0\bar{K}^0}(\mathbf{r}, M_\phi)$ (double-dot–dashed line), $\Gamma_{\phi\to\rho\pi}(\mathbf{r}, M_\phi)$ (dot-dashed line), and $\Gamma_{\rm coll}(\mathbf{r})$ (dashed line) as well as its total width in the medium (solid line) and in the vacuum (dotted line) calculated according to eqs. (11)-(20) at $m_\phi = M_\phi$. It is seen that the partial phi-meson decay widths increase with density if the kaon and rho medium effects are included. After adding to them the collisional width, the resulting total width of the ϕ-meson grows as a function of the density and reaches the value of around 30 MeV for normal nuclear matter density. Note that this value agrees with that obtained in a recent refined hadronic model [76]. The increase in the width of the ϕ-meson would reduce its lifetime in the medium and, hence, may allow it to decay inside the nucleus. Thus, one can easily get the following estimate of the mean free path λ_ϕ of a ϕ-meson with the momentum p_ϕ (*i.e.* the distance which the ϕ has travelled during its lifetime):

$$\lambda_\phi(\mathbf{r}, m_\phi) = \frac{p_\phi}{m_\phi \Gamma_{\rm tot}(\mathbf{r}, m_\phi)}, \tag{22}$$

which has to be compared to the radius[8] of the considered nucleus. So, for the ϕ-meson with a momentum $p_\phi = 100$ MeV/c and at $m_\phi = M_\phi$ one has that $\lambda_\phi \approx 1$ fm at $\Gamma_{\rm tot} = 20$ MeV and $\lambda_\phi \approx 4.4$ fm at $\Gamma_{\rm tot} = 4.45$ MeV. One sees that the first value for λ_ϕ is substantially less than the radius of the ^{63}Cu target nucleus under consideration below, $R \approx 6$ fm. Whereas, for example, at $p_\phi = 1$ GeV/c the mean free path λ_ϕ, as follows from eq. (22) and estimates given above, is greater than the radius of ^{63}Cu for both values of $\Gamma_{\rm tot}$. The foregoing shows that it is essential to apply severe momentum cut to the ϕ three-momentum in order to investigate the sensitivity of observables on the in-medium ϕ properties.

Now let us consider the ϕ production and decay in pA reactions via the production/decay sequences (1, 2) and (1, 3).

2.2 Dikaon and dimuon production cross-sections without including the final-state interactions

Let us first focus on the K^+K^- double differential invariant-mass cross-section arising from (1, 2). Thereafter it is straightforward to get the respective cross-section for the sequence (1, 3). Neglecting the change of the invariant mass of the produced K^+K^- pair due to the kaon final-state interactions (propagation in the Coulomb and the hadronic kaon potentials as well as kaon-nucleon elastic scattering[9]) and taking into consideration the strong absorption of the K^- as well as assuming[10] that the phi-meson spectral function (4) (modified in medium in line with eqs. (11)-(20)) is employed only in its decay to K^+K^- and using the results given in refs. [56,111–115], we can represent the double differential invariant-mass cross-section for the production on nuclei K^+K^- pairs with the invariant mass M_I and total momentum directed along the solid angle $\mathbf{\Omega}_I$ and restricted by the momentum $p_{\rm cut}$ from the secondary decay channel (2) with the slow ϕ produced and going forward[11] in the nuclear lab system as follows:

$$\frac{{\rm d}^2\sigma^{\rm (tot)}_{pA\to K^+K^-X}(\mathbf{p}_0, \mathbf{\Omega}_I \parallel \mathbf{\Omega}_\phi \parallel \mathbf{\Omega}_0)}{{\rm d}M_I {\rm d}\mathbf{\Omega}_I} = \frac{{\rm d}^2\sigma^{\rm (in)}_{pA\to K^+K^-X}(\mathbf{p}_0, \mathbf{\Omega}_I \parallel \mathbf{\Omega}_\phi \parallel \mathbf{\Omega}_0)}{{\rm d}M_I {\rm d}\mathbf{\Omega}_I} + \frac{{\rm d}^2\sigma^{\rm (out)}_{pA\to K^+K^-X}(\mathbf{p}_0, \mathbf{\Omega}_I \parallel \mathbf{\Omega}_\phi \parallel \mathbf{\Omega}_0)}{{\rm d}M_I {\rm d}\mathbf{\Omega}_I}, \tag{23}$$

where

$$\begin{aligned}
&\frac{{\rm d}^2\sigma^{\rm (in)}_{pA\to K^+K^-X}(\mathbf{p}_0, \mathbf{\Omega}_I \parallel \mathbf{\Omega}_\phi \parallel \mathbf{\Omega}_0)}{{\rm d}M_I {\rm d}\mathbf{\Omega}_I} = \\
&2\pi A \int\limits_0^{p_{\rm cut}} p_\phi^2 {\rm d}p_\phi \int\limits_0^R r_\perp {\rm d}r_\perp \\
&\times \int\limits_{-\sqrt{R^2-r_\perp^2}}^{\sqrt{R^2-r_\perp^2}} {\rm d}z \int\limits_0^{\sqrt{R^2-r_\perp^2}-z} {\rm d}x_\parallel \rho(\sqrt{r_\perp^2+z^2}) \\
&\times \exp\left[-\mu(p_0) \int\limits_{-\sqrt{R^2-r_\perp^2}-z}^{0} \rho(\sqrt{r_\perp^2+(z+x)^2}){\rm d}x\right] \\
&\times \left\langle \frac{{\rm d}\sigma_{pN\to pN\phi}(\mathbf{p}_0', m_\phi, p_\phi \mathbf{\Omega}_0)}{{\rm d}\mathbf{p}_\phi} \right\rangle \\
&\times \exp\left[-\int\limits_0^{x_\parallel} \frac{{\rm d}x}{\lambda_\phi(\sqrt{r_\perp^2+(z+x)^2}, m_\phi)}\right] \\
&\times S_\phi(\sqrt{r_\perp^2+(z+x_\parallel)^2}, m_\phi) \\
&\times \Gamma_{\phi\to K^+K^-}(\sqrt{r_\perp^2+(z+x_\parallel)^2}, m_\phi) \\
&\times F_{K^-}^{(abs)}[r_\perp, (z+x_\parallel)]/\gamma_\phi v_\phi,
\end{aligned} \tag{24}$$

[8] It is determined from the relation $\rho_N(R) = 0.03\rho_0$ [52].

[9] The influence of the elastic K^+N and K^-N final-state interactions on the K^+K^- mass spectrum is negligible, since such scattering processes are hindered by Pauli blocking [58, 59] for the low-energy kaons originating from the decays of ϕ with the momenta smaller than 100–150 MeV/c of interest. The effects of the Coulomb and the scalar kaon potentials on this spectrum will be evaluated by us below.

[10] An analogous assumption has been adopted also in ref. [54] to study the dilepton production in π^-A reactions on the basis of the coupled-channel BUU transport model.

[11] A choice of this kinematics has been particularly motivated by the fact that in the threshold energy region ϕ-mesons are mainly emitted in forward direction. It should be noticed that such kinematics has been also used in ref. [58] to calculate the differential cross-section for ϕ photoproduction off nuclei.

$$\frac{\mathrm{d}^2\sigma^{(\mathrm{out})}_{pA\to K^+K^-X}(\mathbf{p}_0,\mathbf{\Omega}_I \parallel \mathbf{\Omega}_\phi \parallel \mathbf{\Omega}_0)}{\mathrm{d}M_I \mathrm{d}\mathbf{\Omega}_I} =$$
$$2\pi A \int\limits_0^{p_{\mathrm{cut}}} p_\phi^2 \mathrm{d}p_\phi \int\limits_0^R r_\perp \mathrm{d}r_\perp \int\limits_{-\sqrt{R^2-r_\perp^2}}^{\sqrt{R^2-r_\perp^2}} \mathrm{d}z \rho(\sqrt{r_\perp^2+z^2})$$
$$\times \exp\left[-\mu(p_0) \int\limits_{-\sqrt{R^2-r_\perp^2}-z}^{0} \rho(\sqrt{r_\perp^2+(z+x)^2})\mathrm{d}x\right]$$
$$\times \left\langle \frac{\mathrm{d}\sigma_{pN\to pN\phi}(\mathbf{p}_0', m_\phi, p_\phi \mathbf{\Omega}_0)}{\mathrm{d}\mathbf{p}_\phi} \right\rangle$$
$$\times \exp\left[- \int\limits_0^{\sqrt{R^2-r_\perp^2}-z} \frac{\mathrm{d}x}{\lambda_\phi(\sqrt{r_\perp^2+(z+x)^2}, m_\phi)}\right]$$
$$\times S_\phi(m_\phi) BR_{\phi\to K^+K^-}(m_\phi) \quad (25)$$

and

$$\left\langle \frac{\mathrm{d}\sigma_{pN\to pN\phi}(\mathbf{p}_0', m_\phi, \mathbf{p}_\phi)}{\mathrm{d}\mathbf{p}_\phi} \right\rangle = \int\int P(\mathbf{p}_t, E)\mathrm{d}\mathbf{p}_t \mathrm{d}E$$
$$\times \left[\frac{\mathrm{d}\sigma_{pN\to pN\phi}(\sqrt{s}, m_\phi, \mathbf{p}_\phi)}{\mathrm{d}\mathbf{p}_\phi}\right], \quad (26)$$

$$F^{(abs)}_{K^-}[r_\perp, (z+x_\parallel)] = \int\limits_0^\pi \sin\theta^*_{K^-} \mathrm{d}\theta^*_{K^-}$$
$$\times \int\limits_0^{2\pi} \mathrm{d}\varphi^*_{K^-} W_{\phi\to K^+K^-}(\theta^*_{K^-}) \theta[E'_{K^-}(\mathbf{r}_{\mathrm{cr}}) - m_{K^-}]$$
$$\times \exp\left[- \int\limits_0^{\sqrt{a^2-b}-a} \mu_{K^-}(\mathbf{r}')\mathrm{d}x\right]; \quad (27)$$

$$r_{\mathrm{cr}} = |\mathbf{r}_{\mathrm{cr}}| = \sqrt{r_\perp^2 + (z+x_\parallel)^2}, \quad (28)$$
$$|\mathbf{r}'| = \sqrt{x^2+2ax+b+R^2},$$
$$a = [(z+x_\parallel)\cos\theta'_{K^-} + r_\perp \sin\theta'_{K^-}\cos\varphi^*_{K^-}],$$
$$b = r_{\mathrm{cr}}^2 - R^2,$$

$$E'_{K^-}(\mathbf{r}_{\mathrm{cr}}) = \gamma_\phi \Big[\overset{*}{E}_{K^-}(\mathbf{r}_{\mathrm{cr}}, m_\phi) + \overset{*}{p}_{K^+K^-}(\mathbf{r}_{\mathrm{cr}}, m_\phi) v_\phi \cos\theta^*_{K^-}\Big],$$
$$\overset{*}{E}_{K^-}(\mathbf{r}_{\mathrm{cr}}, m_\phi) = \sqrt{\overset{*2}{p}_{K^+K^-}(\mathbf{r}_{\mathrm{cr}}, m_\phi) + m^{*2}_{K^-}(\mathbf{r}_{\mathrm{cr}})}, \quad (29)$$

$$\cos\theta'_{K^-} = \gamma_\phi \Big[\overset{*}{p}_{K^+K^-}(\mathbf{r}_{\mathrm{cr}}, m_\phi)\cos\theta^*_{K^-} + \overset{*}{E}_{K^-}(\mathbf{r}_{\mathrm{cr}}, m_\phi) v_\phi\Big] / p'_{K^-}(\mathbf{r}_{\mathrm{cr}}),$$

$$p'_{K^-}(\mathbf{r}_{\mathrm{cr}}) = \sqrt{E'^2_{K^-}(\mathbf{r}_{\mathrm{cr}}) - m^{*2}_{K^-}(\mathbf{r}_{\mathrm{cr}})}, \quad (30)$$

$$\mu(p_0) = \sigma^{\mathrm{in}}_{\mathrm{pp}}(p_0)Z + \sigma^{\mathrm{in}}_{\mathrm{pn}}(p_0)N,\ \mu_{K^-}(\mathbf{r}') = -[2E'_{K^-}(\mathbf{r}_{\mathrm{cr}})\mathrm{Im}U_{K^-}(\mathbf{r}')]/p'_{K^-}(\mathbf{r}'), \quad (31)$$

$$p'_{K^-}(\mathbf{r}') = \sqrt{E'^2_{K^-}(\mathbf{r}_{\mathrm{cr}}) - m^{*2}_{K^-}(\mathbf{r}')}; \quad (32)$$

$$BR_{\phi\to K^+K^-}(m_\phi) = \Gamma_{\phi\to K^+K^-}(m_\phi)/\Gamma_{\mathrm{tot}}(m_\phi), \quad (33)$$

$$\gamma_\phi = E_\phi/m_\phi,\ v_\phi = p_\phi/E_\phi,\ E_\phi = \sqrt{p_\phi^2+m_\phi^2},\ m_\phi = M_I; \quad (34)$$

$$s = (E'_0 + E_t)^2 - (\mathbf{p}'_0 + \mathbf{p}_t)^2, \quad (35)$$

$$E'_0 = E_0 - \frac{\Delta\mathbf{p}^2}{2M_A}, \quad (36)$$

$$\mathbf{p}'_0 = \mathbf{p}_0 - \Delta\mathbf{p}, \quad (37)$$

$$\Delta\mathbf{p} = \frac{E_0 V_0}{p_0}\frac{\mathbf{p}_0}{|\mathbf{p}_0|}, \quad (38)$$

$$E_t = M_A - \sqrt{(-\mathbf{p}_t)^2 + (M_A - m_N + E)^2}. \quad (39)$$

Here, $\mathrm{d}\sigma_{pN\to pN\phi}(\sqrt{s}, m_\phi, \mathbf{p}_\phi)/\mathrm{d}\mathbf{p}_\phi$ is the free differential cross-section for the production of a ϕ-meson with the mass m_ϕ and momentum $\mathbf{p}_\phi$ in reaction (1) at the pN center-of-mass energy $\sqrt{s}$ ($\mathbf{\Omega}_\phi = \mathbf{p}_\phi/p_\phi$); $\rho(\mathbf{r})$, $P(\mathbf{p}_t, E)$ and $W_{\phi\to K^+K^-}(\theta^*_{K^-})$ are the density, nuclear spectral function and K^- angular distribution in the ϕ decay into K^+K^- in its rest frame normalized to unity; $\mathbf{p}_t$ and E are the internal momentum and removal energy of the struck target nucleon just before the collision; $\sigma^{\mathrm{in}}_{pN}$ is the inelastic cross-section of free pN interaction; Z and N are the numbers of protons and neutrons in the target nucleus ($A = N + Z$), M_A is its mass; m_N is the bare nucleon mass; $\mathbf{p}_0$ and E_0 are the momentum and total energy of the initial proton ($\mathbf{\Omega}_0 = \mathbf{p}_0/p_0$); V_0 is the nuclear optical potential that this proton having the kinetic energy T_0 of about a few GeV feels in the interior of the nucleus ($V_0 \approx 40$ MeV); $\mathrm{Im}U_{K^-}$ is the imaginary part of the optical potential which the low-energy antikaon, originating from $\phi \to K^+K^-$ decay, feels inside the nucleus; $\theta(x)$ is the standard step function. The quantities S_ϕ, $\Gamma_{\phi\to K^+K^-}$, $\overset{*}{p}_{K^+K^-}$ and λ_ϕ are defined above by eqs. (4), (12), (14) and (22), respectively.

The first term in eq. (23) describes the contribution to the K^+K^- pair production on nuclei from the decays of ϕ-mesons inside the nucleus (the so-called "inside" component, see fig. 1), whereas the second one represents the contribution to this production from such decays outside the nucleus (the so-called "outside" component). We see that both these contributions are added incoherently in our approach[12]. It is apparent that the corresponding cross-section for the production on nuclei $\mu^+\mu^-$ pairs from the production/decay sequence (1, 3) is governed also

[12] It should be mentioned that the formalism in which the contributions from the decay of the hadron inside and outside the nuclear medium are added coherently, *i.e.* at the amplitude level, has also been developed recently in refs. [116,136,137].

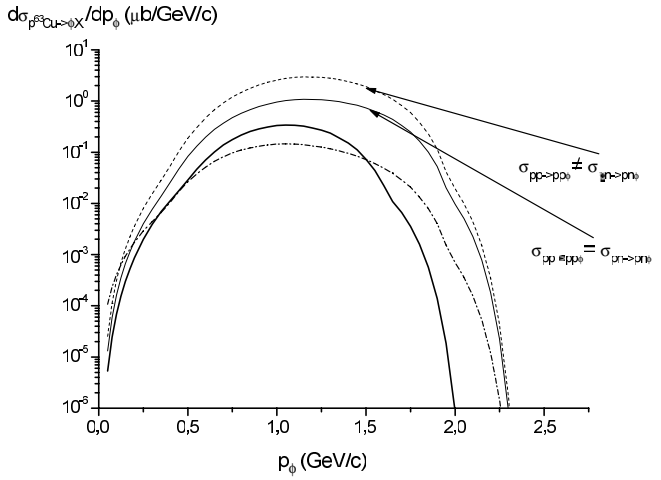

Fig. 3. Momentum differential cross-sections for the production of ϕ-mesons with the pole mass from primary $pN \to pN\phi$ channel in the interaction of protons of energies 2.4 (heavy solid line) and 2.7 GeV (dashed, dot-dashed and light solid lines) with ^{63}Cu nuclei. The heavy and light solid lines are calculations of the momentum distributions of ϕ-mesons which decay outside of this target nucleus without accounting for the difference between the ϕ-meson production cross-sections in pp and pn collisions. The dashed line is the calculation of the momentum distribution of ϕ-mesons which decay also outside of the ^{63}Cu nucleus accounting for the difference between the ϕ-meson production cross-sections in pp and pn interactions in line with ref. [103]. The dot-dashed line is the calculation of the momentum distribution of ϕ-mesons which decay inside the ^{63}Cu nucleus without taking into account this difference. The absorption of phi mesons in nuclear matter was determined by their free width.

by eqs. (23)-(25) in which one has to make the following substitutions: $\Gamma_{\phi\to K^+K^-} \to \Gamma_{\phi\to\mu^+\mu^-}$, $F_{K^-}^{(abs)} \to 1$, $BR_{\phi\to K^+K^-} \to BR_{\phi\to\mu^+\mu^-}$.

In eqs. (24), (25) it is supposed that the ϕ-meson production cross-sections in pp and pn interactions are the same [138][13]. In our calculations of the dikaon (and dimuon) invariant-mass spectra from $p + {}^{12}$C and $p + {}^{63}$Cu collisions reported below these cross-sections have been parametrized according to the three-body phase space (cf. [111]) and were assumed to be isotropic in the pN c.m.s. frame [38,94,99]. The production matrix element squared $|M_{pN\to pN\phi}|^2$ was adjusted to give the data point 0.19 μb for the total cross-section of the reaction $pp \to pp\phi$ from the DISTO Collaboration [99] taken at 83 MeV excess energy. To simplify the calculation of the K^- absorption factor $F_{K^-}^{(abs)}$ given by eq. (27)[14] we assumed in line with ref. [139] that the antikaon angular distribution $W_{\phi\to K^+K^-}(\theta^*_{K^-})$ in the ϕ rest frame is isotropic[15] and used the following parametrization for the imaginary part of the low-energy K^- optical potential, which has been obtained in ref. [121] within a self-consistent microscopic approach:

$$\mathrm{Im}U_{K^-}(\mathbf{r}) = -100\left(\frac{\rho_N(\mathbf{r})}{\rho_0}\right) + 52\left(\frac{\rho_N(\mathbf{r})}{\rho_0}\right)^2 \text{ MeV}. \quad (40)$$

For the K^+K^- ($\mu^+\mu^-$) production calculations in the case of the ^{12}C and ^{63}Cu target nuclei reported here we have employed for the nuclear density $\rho(\mathbf{r})$, respectively, the harmonic oscillator and a two-parameter Fermi density distributions:

$$\rho(\mathbf{r}) = \rho_N(\mathbf{r})/A = \frac{(b/\pi)^{3/2}}{A/4} \times \left\{1 + \left[\frac{A-4}{6}\right] br^2\right\} \exp\left(-br^2\right), \quad (41)$$

$$\rho(\mathbf{r}) = \rho_0 \left[1 + \exp\left(\frac{r - R_{1/2}}{a}\right)\right]^{-1} \quad (42)$$

with $b = 0.355$ fm^{-2} [120] and $R_{1/2} = 4.20$ fm, $a = 0.55$ fm [114]. The nuclear spectral function $P(\mathbf{p}_t, E)$ (which represents the probability to find a nucleon with momentum $\mathbf{p}_t$ and removal energy E in the nucleus) for these target nuclei was taken from refs. [111–114].

Now, let us proceed to the discussion of the results of our calculations for production and decay of ϕ-mesons in p^{12}C and p^{63}Cu interactions in the framework of the model outlined above.

At first, we consider the momentum differential cross-sections for ϕ production from ^{63}Cu calculated on the basis of eqs. (24), (25) and depicted in fig. 3. In this plot we show four different curves, corresponding to various beam energies and different scenarios: three curves correspond to calculations of the momentum distributions of ϕ-mesons which decay outside of the ^{63}Cu nucleus at 2.4 and 2.7 GeV incident laboratory kinetic energies and one curve belongs to the calculation of the momentum distribution of ϕ-mesons which decay inside this target nucleus at 2.7 GeV initial energy. For the first case we show calculations with and without taking into account the difference between the ϕ-meson production cross-sections in pp and pn interactions. Comparing the curves, corresponding to the momentum distributions of ϕ-mesons decaying inside and outside of the ^{63}Cu nucleus (dot-dashed and light solid lines, respectively), we see that in the region of low ϕ momenta ($p_\phi \leq 100$ MeV/c) the contribution of in-medium decays is larger than that from vacuum decays (they differ by a factor of about 2.5 at ϕ momentum of 100 MeV/c, while at momentum of 50 MeV/c the difference between them is up to one order of magnitude).

[13] Later on, in order to get an estimate on the possible uncertainty of our calculations due to the poor knowledge of these cross-sections in the threshold energy region, they will be taken also different [83,84] when calculating the momentum differential cross-section for ϕ production from ^{63}Cu (see fig. 3).

[14] It should be noted that the step function in this equation accounts for the additional absorption of the ϕ daughter low-energy K^--meson in nuclear matter in case its total energy is smaller than its vacuum mass. Therefore, such a K^- cannot escape from the nucleus and finally will be absorbed inside the nucleus in channels like $K^-N \to \pi Y$.

[15] We have checked that an anisotropic distribution (proportional to $\sin^2\theta^*_{K^-}$ [84,85]) has no significant influence on our results.

Whereas, fast ϕ's mainly decay in the vacuum. Thus, it is clear that in order to study in-medium decays of ϕ-mesons their momenta have to be restricted to very small values.

In order to get an estimate of the possible uncertainty of our calculations due to the poor knowledge of the cross-sections of the reactions $pp \to pp\phi$ and $pn \to pn\phi$ in the threshold energy region we performed additional calculations where we adopted for these cross-sections the parametrizations from ref. [103]. These parametrizations were obtained on the basis of the results of calculations [83,84] of the ϕ production cross-sections from pp and pn interactions within the one-boson exchange model. They show particularly that the total cross-section for the pn reaction is greater by a factor of about 5 than the one of the pp reaction in the near-threshold energy region. The results are shown also in fig. 3 (dashed line). Comparing these results with those obtained without accounting for the difference between the ϕ-meson production cross-sections in pp and pn collisions (light solid line), we find an enhancement of the spectrum by a factor of about 2.0–2.5 when the respective parametrizations from ref. [103] are employed. Hence, it is believed that the possible error of our calculations due to the elementary ϕ production cross-sections is of the order of this factor. Further, one can also see that the values of the ϕ production cross-section on ^{63}Cu in the low-momentum region of our interest are very small and they increase only by a factor of about 2.3 when the beam energy increases from $T_0 = 2.4$ GeV to $T_0 = 2.7$ GeV (compare heavy and light solid lines). The small strength of this cross-section in the range of low ϕ momenta is caused by the fact that due to the kinematics the production of such phi mesons in the free nucleon-nucleon interactions is strongly forbidden in the energy regime under consideration and, therefore, high internal nucleon momenta are needed to allow the low-momentum ϕ production in the direct process (1) in this regime. Thus, for example, our calculations show that the free threshold energy for the production of a ϕ-meson with momentum of 150 MeV/c at a laboratory angle of 0° from the process $pN \to pN\phi$ is equal to 22.05 GeV! As a result, the minimal internal nucleon momenta needed for ϕ production in this process taking place on a nucleon embedded in a ^{63}Cu target nucleus at incident energies of 2.4 and 2.7 GeV turn out to be equal to 425 and 375 MeV/c, respectively. Note that the behavior of the nuclear spectral function[16] at such high values of the nucleon momentum is almost entirely governed by its correlated part [111,140,141] generated in the ground state of the target nucleus by NN correlations. In order to get a deeper insight into the allowed momenta of ϕ-mesons in the processes $pp \to pp\phi$ and $p\mathrm{Cu} \to p\mathrm{Cu}\phi$ at initial energy of 2.7 GeV, we calculated the ellipses of phi momenta in these processes at given beam energy. The results of calculations are shown in fig. 4. It is clearly seen that the ϕ momenta smaller than 0.93 GeV/c are not allowed by the kinematics in the free proton-proton interactions at 2.7 GeV incident energy, whereas they are accessible in pCu collisions.

[16] Which is responsible for the ϕ-meson production in the proton-induced reaction channel (1), see eq. (26).

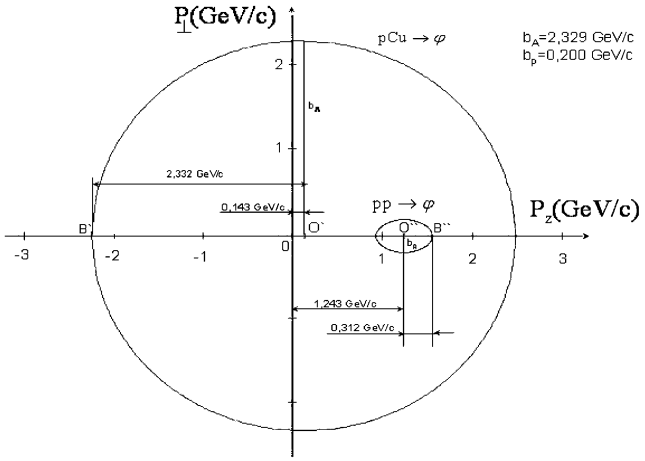

Fig. 4. The ellipses of the allowed by the kinematics ϕ momenta in the processes $pp \to pp\phi$ and $p\mathrm{Cu} \to p\mathrm{Cu}\phi$ at initial energy of 2.7 GeV. p_z and $p_\perp$ represent the longitudinal and transverse momenta of the produced ϕ-meson in the lab system, respectively. The accessible phi three-momenta in the reactions $pp \to pp\phi$ and $p\mathrm{Cu} \to p\mathrm{Cu}\phi$ lie inside the corresponding ellipses, whereas the inaccessible ones locate outside these ellipses.

Let us concentrate now on the dikaon and dimuon invariant-mass spectra arising, correspondingly, from the production/decay channels (1, 2) and (1, 3).

Figure 5 shows double differential invariant-mass cross-sections calculated by eqs. (24) and (25) within the different scenarios for the production of K^+K^- pairs from the decays of ϕ-mesons inside and outside of the ^{12}C target nuclei in the interaction of protons with laboratory kinetic energy of 2.4 GeV with these nuclei. The results of our overall calculations (the sum of contributions from ϕ decays both inside and outside of the ^{12}C nuclei depicted in fig. 5) are presented in fig. 6. One can see that the width of the K^+K^- invariant-mass spectrum from in-medium decays of ϕ-mesons with modified spectral function reacts weakly to the momentum cutoff parameter p_{cut}, whereas its strength depends strongly on this parameter, namely, a smaller momentum cut reduces significantly the strength of the cross-section in the vicinity of the ϕ-meson pole mass (compare dashed and solid lines on the left in fig. 5). A moderate sensitivity of the width of this spectrum to the momentum cutoff p_{cut} can be explained by the fact that the events which yield the broadening of the spectrum, *i.e.* the events stemming from ϕ decays at finite densities (the relative number of which is increased with decreasing the momentum cut), are reduced substantially by the rather strong absorption of the final-state antikaons. Therefore, the main contribution to the invariant-mass spectrum comes from phi decays in the nuclear surface. This leads to a width of the spectrum of about 8 MeV, which is nearly twice the width of the K^+K^- invariant-mass distribution from in-medium decays of ϕ-mesons with vacuum spectral function (dot-dashed line on the left in fig. 5). Figure 5 also shows that the K^+K^- invariant-mass cross-sections for the outside component (depicted on the right in this

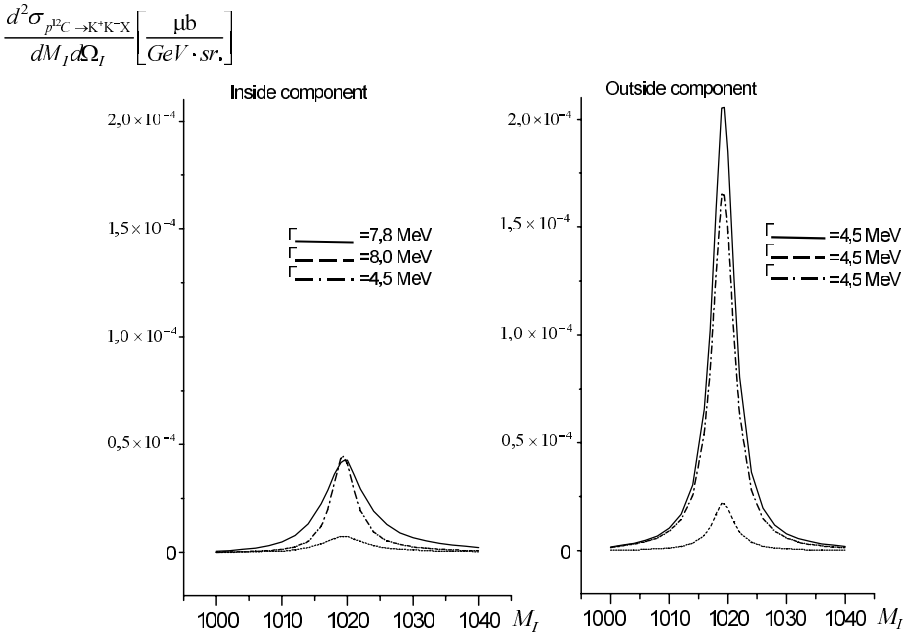

Fig. 5. Double differential invariant-mass cross-sections for the production of K^+K^- pairs from the decays of ϕ-mesons going forward in the nuclear lab frame inside (left panel) and outside (right panel) of the ^{12}C target nuclei in the interaction of 2.4 GeV protons with these nuclei. The dot-dashed and solid lines are calculations at $p_{\rm cut} = 150$ MeV/c, $U_K(\rho_N) = 0$, $U_{\bar{K}}(\rho_N) = 0$, $\alpha_\rho = 0$, $\Gamma_{\rm coll} = 0$ and $p_{\rm cut} = 150$ MeV/c, $U_K(\rho_N) = 22(\rho_N/\rho_0)$ MeV, $U_{\bar{K}}(\rho_N) = -126(\rho_N/\rho_0)$ MeV, $\alpha_\rho = 0.18$, $\Gamma_{\rm coll} = 10(\rho_N/\rho_0)$ MeV, respectively. The dashed line denotes the same as the solid line, but $p_{\rm cut} = 100$ MeV/c. The dot-dashed line is one-third of the cross-section calculated using the corresponding parameters which are indicated above. The quantity Γ with the line placed on the lower right of it denotes the full width at half-maximum of the mass spectrum presented by the same line in the figure. The invariant mass M_I here and in the following figures is measured in MeV.

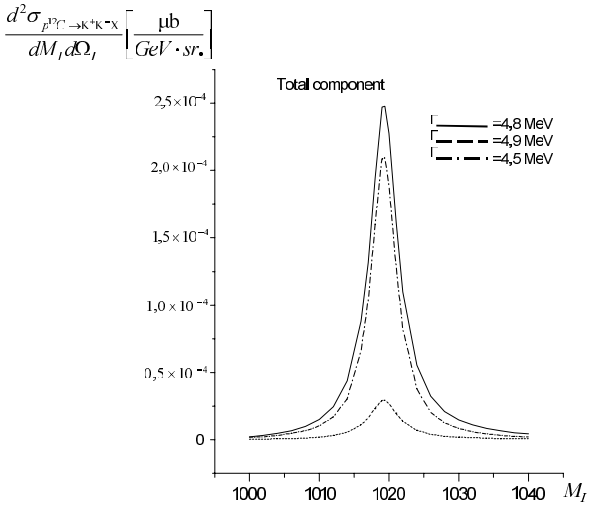

Fig. 6. Double differential invariant-mass cross-sections for the production of K^+K^- pairs from the decays of ϕ-mesons going forward in the nuclear lab frame both inside and outside of the ^{12}C target nuclei in the interaction of 2.4 GeV protons with these nuclei. The notation of the curves is identical to that in fig. 5.

figure), calculated using the same scenarios for the width of ϕ-mesons when they travel to the vacuum and for the momentum cutoff parameter $p_{\rm cut}$ as those adopted in the preceding case, have, as would be expected, the free phi width. It is nicely seen that their strengths are essentially larger than the ones of the respective cross-sections for the inside component presented on the left in fig. 5. As a consequence, the full K^+K^- invariant-mass distribution (shown in fig. 6) which corresponds to calculations where the modification of the ϕ-meson in nuclear matter is taken into account has a width (~ 4.8 MeV) very close to the free one (compare dashed, solid and dot-dashed lines) and this width is rather insensitive to the ϕ momentum cut (compare dashed and solid lines). This means that it will be quite difficult to measure such small deviations of the mass distribution compared to the situation in free space on light nuclei in proton-induced reactions, looking for K^+K^- pairs from the ϕ decay with total momentum smaller than 100–150 MeV/c even employing the detectors with high mass resolution.

Figure 7 presents double differential invariant-mass cross-sections calculated on the basis of eqs. (24) and (25) within the different scenarios for the production of $\mu^+\mu^-$ pairs from the decays of ϕ-mesons inside and outside of the ^{12}C target nuclei in the interaction of 2.4 GeV protons with these nuclei. The results of our full calculations (the sum of the inside and outside components displayed in fig. 7) are given in fig. 8. It can be seen that the dropping of $m_K^* + m_{\bar{K}}^*$ and M_ρ^* scenario as well as the inclusion of collisional broadening of ϕ-mesons due to their two-body collisions with nucleons in the nuclear environment and

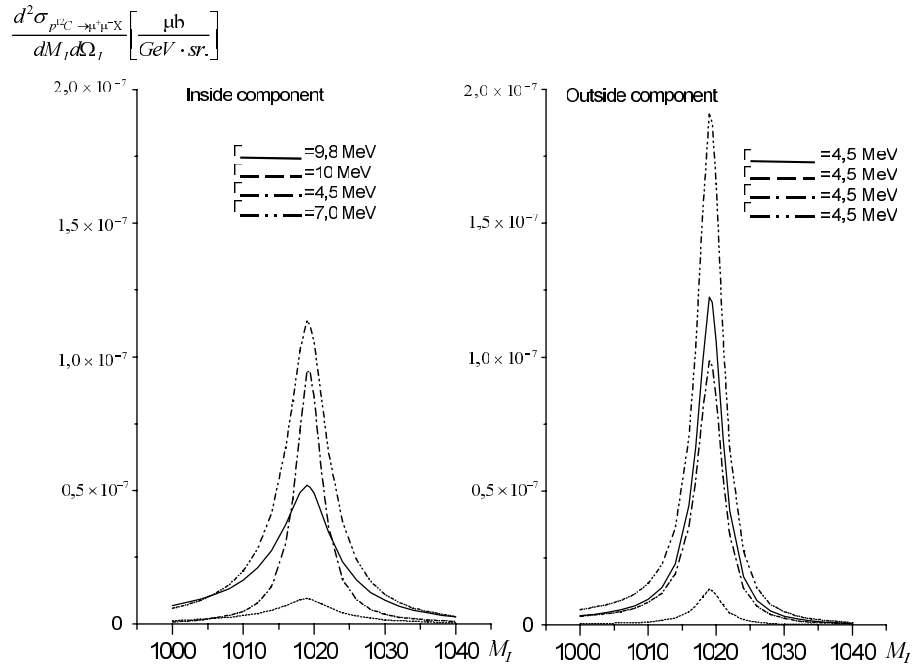

Fig. 7. Double differential invariant-mass cross-sections for the production of $\mu^+\mu^-$ pairs from the decays of ϕ-mesons going forward in the nuclear lab frame inside (left panel) and outside (right panel) of the ^{12}C target nuclei in the interaction of 2.4 GeV protons with these nuclei. The double-dot–dashed line is the calculation at $p_{\rm cut} = 150$ MeV/c, $U_K(\rho_N) = 0$, $U_{\bar{K}}(\rho_N) = 0$, $\alpha_\rho = 0$, $\Gamma_{\rm coll} = 10(\rho_N/\rho_0)$ MeV. The rest of the notation is identical to that in fig. 5.

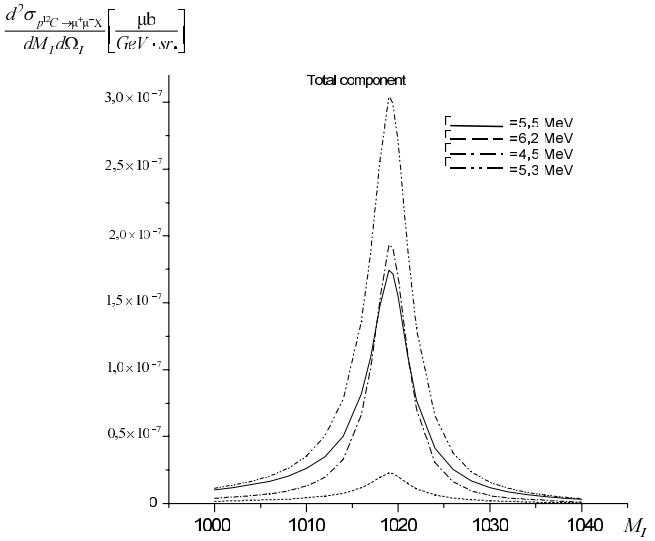

Fig. 8. Double differential invariant-mass cross-sections for the production of $\mu^+\mu^-$ pairs from the decays of ϕ-mesons going forward in the nuclear lab frame both inside and outside of the ^{12}C target nuclei in the interaction of 2.4 GeV protons with these nuclei. The notation of the curves is identical to that in fig. 7.

the cuts of 100 and 150 MeV/c in their momenta lead to the $\mu^+\mu^-$ invariant-mass distributions from in-medium decays of phi mesons (dashed and solid lines on the left in fig. 7) which are wider than the corresponding K^+K^- invariant-mass spectra presented on the left in fig. 5. We observe in this case that the widths of these distributions are also approximately equal in magnitude and amount to $\approx$ 10 MeV. The increase of these widths compared to those found in the K^+K^- pair production case can be explained by the larger sensitivity of the calculated $\mu^+\mu^-$ mass spectra to the nuclear interior (where the ϕ width is enhanced, see fig. 2) due to the lack of the absorption of the final-state muons. On the other hand, since the sum of the mean free paths of initial proton and primarily produced slow ϕ-meson is comparable to the radius of the considered target nucleus, most of the phi mesons still decay in the nuclear surface even if the different cuts of 100 and 150 MeV/c in their momenta are applied. This causes an approximate equality of these widths. But the use of the momentum cut of 100 MeV/c reduces significantly the cross-section. One can also see that the inclusion of only collisional broadening of ϕ-mesons alone (double-dot–dashed line on the left in fig. 7) leads to a moderate broadening of the dimuon yield from their decays inside the nucleus under consideration compared to that (dot-dashed line) calculated using the free spectral function of the ϕ. Comparing figs. 5 and 7, we see very nicely that the ratios of the dimuon yields from ϕ decays inside and outside of the ^{12}C nucleus calculated with allowance for the different scenarios for the ϕ width and momentum cut are enhanced (by a factor of about three) compared to the respective ratios of the dikaon yields from this target nucleus. As a result, the full $\mu^+\mu^-$ invariant-mass distributions (shown in fig. 8) which correspond to calculations for the momentum cuts of 100 and 150 MeV/c, where the kaon and

ρ-meson mass shifts as well as the collisional broadening of ϕ-mesons are taken into account, are wider than the respective total K^+K^- invariant-mass spectra (compare dashed and solid lines in figs. 6 and 8). We observe that the widths of these distributions are 6.2 MeV ($p_{\rm cut}$ = 100 MeV/c) and 5.5 MeV ($p_{\rm cut}$ = 150 MeV/c). Owing to collisional broadening alone, the width of the resulting $\mu^+\mu^-$ invariant-mass spectrum (double-dot–dashed line in fig. 8) increases in relation to the free ϕ width only of 0.8 MeV and amounts to 5.3 MeV. Comparing these values with the free ϕ width (4.5 MeV), we see that the use of the adopted in-medium phi widths and the cuts of 100 and 150 MeV/c in the phi momenta leads to only moderate broadening of the $\mu^+\mu^-$ invariant-mass spectra from the decays of primarily produced ϕ-mesons in pC interactions at 2.4 GeV beam energy which is comparable to that found earlier in the case of K^+K^- invariant-mass distributions. This means that it will be also quite difficult to observe the effect of ϕ in-medium broadening through the $\mu^+\mu^-$ invariant-mass spectrum using ^{12}C as target nucleus at the employed incident energy. On the other hand, the height of the peak in this spectrum around the vacuum pole mass M_ϕ of the ϕ-meson, as can be seen from fig. 8, is strongly affected by the employed scenario for its width in the medium[17]. Thus, for a momentum cut of 150 MeV/c, a collisional broadening scenario alone results in reduction of the dimuon yield here compared to that calculated using the free ϕ width by a factor of about 2 (compare dot-dashed and double-dot–dashed lines). An additional inclusion of the kaon and rho mass shifts reduces the cross-section yet by a factor of about 1.5 (compare double-dot–dashed and solid lines). However, this strong sensitivity of the dimuon yield for masses around the vacuum pole mass to the ϕ in-medium spectral function apparently cannot help to discriminate experimentally between different scenarios for its properties inside the nuclear matter due to the uncertainties of the cross-sections for phi production in pN collisions implemented.

Figure 9 shows double differential invariant-mass cross-sections for the production of K^+K^- pairs from the decays of primarily produced ϕ-mesons inside and outside of the ^{63}Cu target nuclei in the interaction of 2.4 GeV protons with these nuclei calculated with allowance for the same scenarios for the ϕ width and momentum cut as in the preceding case, while fig. 10 presents the sum of the "in" and "out" components depicted in fig. 9. Comparing figs. 5 and 9, we see that the simultaneous inclusion of the kaon and rho-meson mass shifts as well as the phi collisional broadening and an application of the cuts of 100 and 150 MeV/c in the ϕ momentum lead to the K^+K^- invariant-mass distributions from in-medium decays of ϕ-mesons whose widths in the case of having ^{63}Cu as target nucleus are approximately equal to those found for the ^{12}C target nuclei. This is caused by the fact that the calculated dikaon mass spectra are merely sensitive to the nuclear surface[18] due to the rather strong absorption of the final-state antikaons in nuclear matter. As in the case of ^{12}C target nuclei, for ^{63}Cu nucleus the "outside" dikaon mass distributions are also larger than the respective "inside" K^+K^- mass spectra in all considered scenarios for the phi width and momentum cut. As a result, the K^+K^- invariant-mass spectra from ϕ-mesons decaying both inside and outside of the ^{63}Cu nucleus (shown in fig. 10) calculated for the momentum cuts of 100 and 150 MeV/c including the kaon and ρ meson mass shifts as well as the phi collisional broadening, are only slightly broader than the corresponding total dikaon invariant-mass distributions obtained in the case of having ^{12}C as target nucleus (compare dashed and solid lines in figs. 6 and 10). We can see that the widths of these spectra are 5.2 and 4.9 MeV for the momentum cuts of 100 and 150 MeV/c, respectively. With the inclusion of collisional broadening alone the width of the resulting K^+K^- invariant-mass spectrum (double-dot–dashed line in fig. 10) is smaller than the above ones and it equals 4.7 MeV. All these widths are also comparable in magnitude to the free phi width.

Thus, our model calculations do not indicate an observable broadening of the K^+K^- invariant-mass spectrum due to the ϕ in-medium width also from p + ^{63}Cu collisions at 2.4 GeV beam energy. Since the calculated spectrum is sensitive mainly to the nuclear surface because of the strong absorption of the K^- in nuclear matter, we expect to get an analogous broadening of the dikaon invariant-mass distribution due to the in-medium width of the phi also in the case of heavy target nuclei. This means that the experimental observation of sizeable changes in the nuclear shape of the ϕ reconstructed from the K^+K^- pairs should require another explanation of these changes, for example, that based on the change of momenta of daughter kaons due to the Coulomb and the hadronic kaon potentials when they propagate from the interior of a nucleus to the vacuum. The effects of these potentials on the dikaon invariant-mass distribution in p^{63}Cu reactions will be estimated in the next section.

We, therefore, come to the conclusion that the in-medium properties of the phi will be hard to observe through the K^+K^- invariant-mass spectrum, at least, at the density of ordinary nuclei.

Finally, fig. 11 demonstrates double differential invariant-mass cross-sections for the production of $\mu^+\mu^-$ pairs from the decays of primarily produced ϕ-mesons inside and outside of the ^{63}Cu target nuclei in the interaction of 2.4 GeV protons with these nuclei calculated with allowance for the same scenarios for the ϕ width and momentum cut as those of figs. 9, 10, while fig. 12 shows the sum of the "in" and "out" components displayed in fig. 11. One can see that the inclusion of the kaon and ρ-meson mass shifts as well as the ϕ collisional broadening and

[17] It should be pointed out that our previous findings of fig. 6 show also strong sensitivity of the dikaon production cross-section for masses around M_ϕ to the in-medium phi width. Therewithal, the strength of this cross-section here, as is seen from the comparison of figs. 6 and 8, is three orders of magnitude greater than the one of the cross-section for dimuon production.

[18] Thus, our calculations showed that the 90% contribution to the dikaon invariant-mass spectra from ϕ decays inside the ^{63}Cu nucleus comes from nuclear densities $\rho < 0.2\rho_0$.

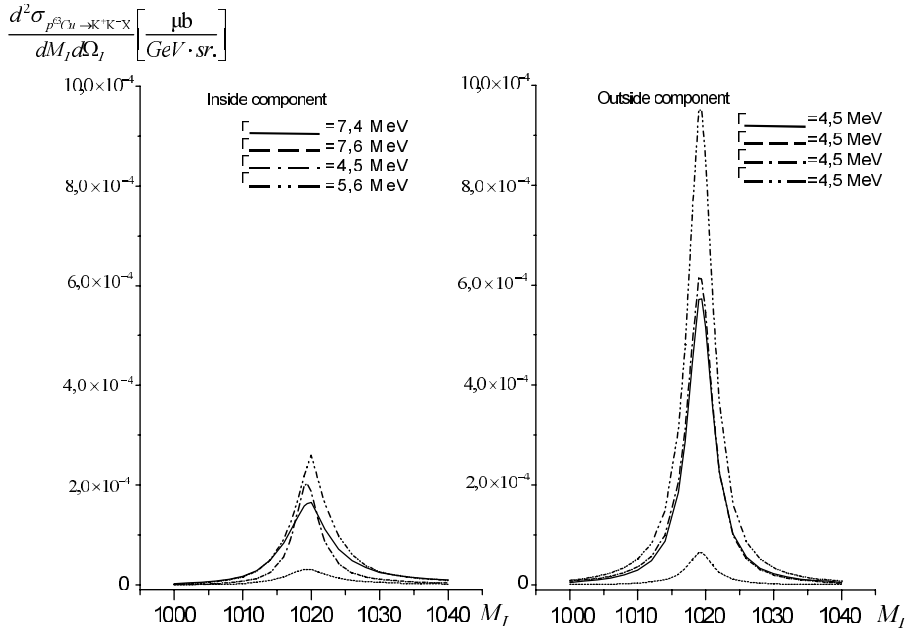

Fig. 9. Double differential invariant-mass cross-sections for the production of K^+K^- pairs from the decays of ϕ-mesons going forward in the nuclear lab frame inside (left panel) and outside (right panel) of the ^{63}Cu target nuclei in the interaction of 2.4 GeV protons with these nuclei. The double-dot–dashed line is the calculation at $p_{\rm cut} = 150$ MeV/c, $U_K(\rho_N) = 0$, $U_{\bar{K}}(\rho_N) = 0$, $\alpha_\rho = 0$, $\Gamma_{\rm coll} = 10(\rho_N/\rho_0)$ MeV. The rest of the notation is identical to that in fig. 5.

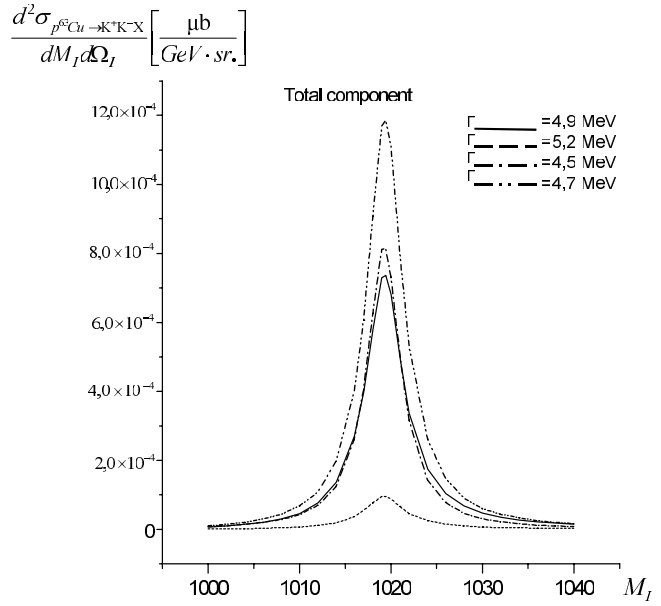

Fig. 10. Double differential invariant-mass cross-sections for the production of K^+K^- pairs from the decays of ϕ-mesons going forward in the nuclear lab frame both inside and outside of the ^{63}Cu target nuclei in the interaction of 2.4 GeV protons with these nuclei. The notation of the curves is identical to that in fig. 9.

low-momentum cuts leads to the dimuon invariant-mass spectra from in-medium decays of phi mesons (dashed and solid lines on the left in fig. 11) which are broader than the respective $\mu^+\mu^-$ mass distributions from the ^{12}C target nucleus (cf. fig. 7). We find that the widths of these spectra are also approximately equal in magnitude and amount to ≈ 10.5 MeV. With the inclusion of collisional broadening alone the width of the dimuon yield from ϕ decays inside the ^{63}Cu target nucleus, as can be seen from fig. 11, is smaller than the above ones and it equals 7.7 MeV. Comparing figs. 7 and 11, we observe that the relative weight of the inside decay component relative to the vacuum component increases by about a factor of 2 in all adopted scenarios for the phi width and momentum cut when going from ^{12}C to ^{63}Cu. As a consequence, the full $\mu^+\mu^-$ invariant-mass distributions (presented in fig. 12) calculated for the momentum cuts of 100 and 150 MeV/c including the kaon and rho-meson mass shifts as well as the ϕ collisional broadening are wider than the corresponding total dimuon mass spectra obtained in the case of the ^{12}C target nucleus (compare dashed and solid lines in figs. 8 and 12). One sees that the widths of these distributions are 7.5 and 6.4 MeV for the momentum cuts of 100 and 150 MeV/c, respectively. The first magnitude is nearly twice the free phi width. This change in the nuclear width of the ϕ should be in principle measurable using the detectors with high mass resolution. As would be expected, the collisional broadening scenario alone (double-dot–dashed line in fig. 12) gives only a moderate increase (by about a factor of 1.3) of the width of the resulting dimuon mass spectrum compared to the free ϕ width, which will be hard to see experimentally.

Thus, our results show an observable enhancement of the width of the resulting $\mu^+\mu^-$ invariant-mass distribution due to the total phi in-medium width by a factor of about 2 from $p +$ ^{63}Cu reactions at 2.4 GeV incident

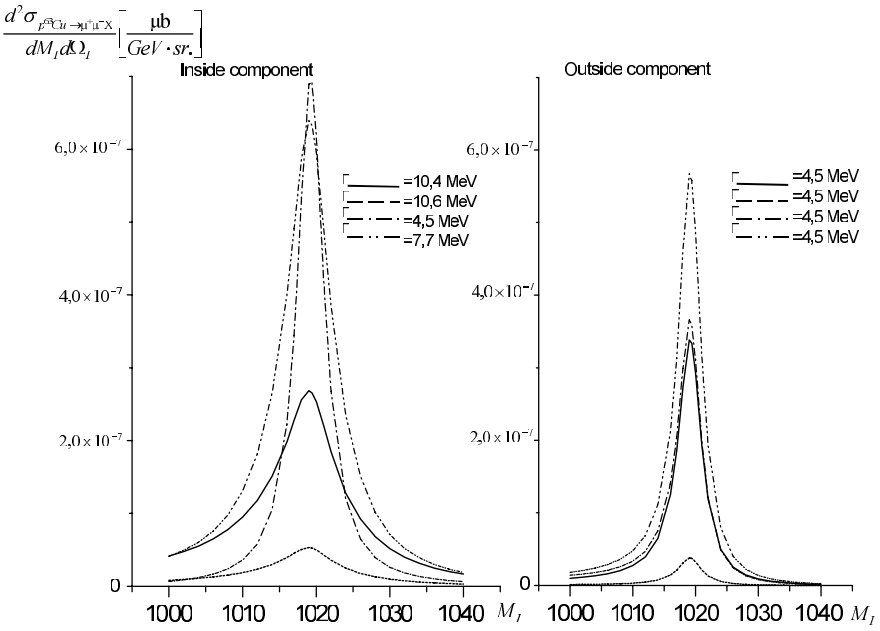

Fig. 11. Double differential invariant-mass cross-sections for the production of $\mu^+\mu^-$ pairs from the decays of ϕ-mesons going forward in the nuclear lab frame inside (left panel) and outside (right panel) of the ^{63}Cu target nuclei in the interaction of 2.4 GeV protons with these nuclei. The double-dot–dashed line is the calculation at $p_{\rm cut} = 150$ MeV/c, $U_K(\rho_N) = 0$, $U_{\bar{K}}(\rho_N) = 0$, $\alpha_\rho = 0$, $\Gamma_{\rm coll} = 10(\rho_N/\rho_0)$ MeV. The rest of the notation is identical to that in fig. 5.

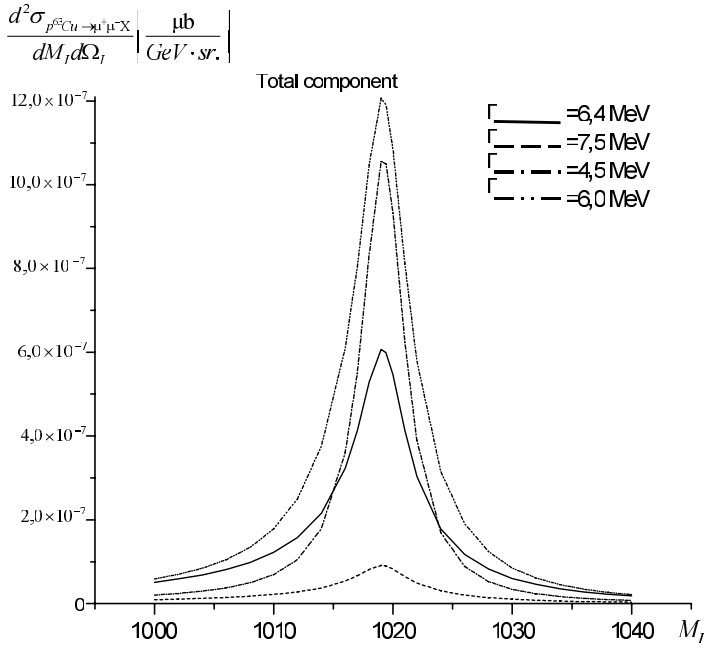

Fig. 12. Double differential invariant-mass cross-sections for the production of $\mu^+\mu^-$ pairs from the decays of ϕ-mesons going forward in the nuclear lab frame both inside and outside of the ^{63}Cu target nuclei in the interaction of 2.4 GeV protons with these nuclei. The notation of the curves is identical to that in fig. 11.

energy when applying the momentum cut of 100 MeV/c. The enhancement is expected to be even larger for heavier target nuclei, since the relative weight of the dimuon "inside" component relative to the "outside" component, as showed by our calculations, increases with A. This gives the opportunity to study the in-medium properties of the ϕ at finite baryon density experimentally by measuring for low-momentum cuts the dilepton yields from the decays of phi mesons produced in the interaction of protons with medium and heavy target nuclei[19].

[19] Note that in our analysis we did not consider the ϕ dilepton decay signal to background ratio. This ratio was found [52] to be large for π^-Pb reactions at 1.7 GeV/c. Since the ϕ is a very narrow resonance and we therefore look only on a very limited region invariant masses around the pole mass M_ϕ, it is natural

Let us focus now on the estimate of the impact of the Coulomb and the hadronic kaon potentials on the K^+K^- invariant-mass spectrum.

2.3 Dikaon production cross-section including the kaon final-state interactions

The Coulomb and the scalar kaon potentials (18) modify the invariant mass of the K^+K^- pair, resulting from the decay of a slow ϕ-meson, as this pair propagates from the creation point into the vacuum. As a consequence, the invariant mass M_I, reconstructed from the kaon pair, deviates from the mass m_ϕ of the decayed phi meson. Assuming for simplicity that the directions of the kaon three-momenta remain unchanged as well as considering that the single-particle energies are constants of motion and the momentum cutoff $p_{\rm cut}$ is applied to the three-momentum of the K^+K^- pair, we can rewrite expression (24) for the "inside" component of the dikaon invariant-mass spectrum in the following form, which includes approximately also the effect of the kaon potentials on the propagation of kaons and antikaons:

$$\frac{{\rm d}^2\sigma^{\rm (in)}_{pA\to K^+K^-X}(\mathbf{p}_0,\mathbf{\Omega}_I \parallel \mathbf{\Omega}_\phi \parallel \mathbf{\Omega}_0)}{{\rm d}M_I {\rm d}\mathbf{\Omega}_I} =$$

$$2\pi A \int\limits_0^R r_\perp {\rm d}r_\perp \int\limits_{-\sqrt{R^2-r_\perp^2}}^{\sqrt{R^2-r_\perp^2}} {\rm d}z \int\limits_0^{\sqrt{R^2-r_\perp^2}-z} {\rm d}x_\parallel \int p_\phi^2 {\rm d}p_\phi$$

$$\times \int\limits_{m^*_{K^+}+m^*_{K^-}}^{\sqrt{s}-2m_N} {\rm d}m_\phi \rho(\sqrt{r_\perp^2+z^2})$$

$$\times\theta\left[p_{\rm cut}^2+\left(M_I^2-m_\phi^2\right)-p_\phi^2\right]\ \delta\left(M_I-m_\phi-\overline{\Delta m}\right)$$

$$\times \exp\left[-\mu(p_0)\int\limits_{-\sqrt{R^2-r_\perp^2}-z}^{0}\rho(\sqrt{r_\perp^2+(z+x)^2}){\rm d}x\right]$$

$$\times\left\langle\frac{{\rm d}\sigma_{pN\to pN\phi}(\mathbf{p}'_0,m_\phi,p_\phi\mathbf{\Omega}_0)}{{\rm d}\mathbf{p}_\phi}\right\rangle$$

$$\times \exp\left[-\int\limits_0^{x_\parallel}\frac{{\rm d}x}{\lambda_\phi(\sqrt{r_\perp^2+(z+x)^2},m_\phi)}\right]$$

$$\times S_\phi(\sqrt{r_\perp^2+(z+x_\parallel)^2},m_\phi)$$

$$\times \Gamma_{\phi\to K^+K^-}(\sqrt{r_\perp^2+(z+x_\parallel)^2},m_\phi)$$

$$\times F^{(abs)}_{K^-}[r_\perp,(z+x_\parallel)]/\gamma_\phi v_\phi. \qquad (43)$$

to expect that this signal can be distinguished from the dominant background from the ρ decay in the case of pA collisions as well. The ϕ signal to background ratio was found [24] to be large also for K^+K^- pairs in these collisions.

Here, $\overline{\Delta m}$ is the average over all possible directions for the K^+ and K^- invariant-mass shift of the K^+K^- pair due to the kaon potentials when this pair propagates from its creation point $\mathbf{r}_{\rm cr}$ ($|\mathbf{r}_{\rm cr}|=\sqrt{r_\perp^2+(z+x_\parallel)^2}$) inside the nucleus to the vacuum far away from the nucleus.

Let us now specify the quantity $\overline{\Delta m}$. As is easy to see, the modification of the invariant mass of the K^+K^- pair in the general case can be written as

$$\Delta m=\frac{(\mathbf{p}'_{K^+}+\mathbf{p}'_{K^-})^2-(\mathbf{p}_{K^+}+\mathbf{p}_{K^-})^2}{2m_\phi}, \qquad (44)$$

where $\mathbf{p}'_{K^\pm}$ and $\mathbf{p}_{K^\pm}$ are the in-medium (at the creation point) and the vacuum three-momenta of K^+/K^-, respectively. Taking into consideration that the absolute values of the K^+/K^- three-momenta in vacuum are given by

$$|\mathbf{p}_{K^\pm}|=|\mathbf{p}'_{K^\pm}|\sqrt{1+\left[m^{*2}_{K^\pm}(\mathbf{r}_{\rm cr})-m_K^2\right]/|\mathbf{p}'_{K^\pm}|^2} \qquad (45)$$

and assuming in line with the above mentioned that these momenta are parallel to the in-medium ones $\mathbf{p}'_{K^\pm}$, we can readily rewrite eq. (44) in the form

$$\Delta m=-\frac{1}{2m_\phi}(I_1+I_2), \qquad (46)$$

where

$$I_1=\frac{2\mathbf{p}_\phi\mathbf{p}'_{K^+}\Delta_+}{|\mathbf{p}'_{K^+}|^2a_+}+\frac{2\mathbf{p}_\phi\mathbf{p}'_{K^-}\Delta_-}{|\mathbf{p}'_{K^-}|^2a_-}, \qquad (47)$$

$$I_2=\left(\frac{\mathbf{p}'_{K^+}\Delta_+}{|\mathbf{p}'_{K^+}|^2a_+}+\frac{\mathbf{p}'_{K^-}\Delta_-}{|\mathbf{p}'_{K^-}|^2a_-}\right)^2 \qquad (48)$$

and

$$\Delta_\pm=m^{*2}_{K^\pm}(\mathbf{r}_{\rm cr})-m_K^2,\quad a_\pm=1+\sqrt{1+\Delta_\pm/|\mathbf{p}'_{K^\pm}|^2}. \qquad (49)$$

Finally, taking into account that in the limit case $p_\phi\le \overset{*}{p}_{K^+K^-}$ of our interest the kaon momenta $\mathbf{p}'_{K^\pm}$ can be approximately expressed as [43]

$$\mathbf{p}'_{K^\pm}=\frac{\mathbf{p}_\phi}{2}\mp \overset{*}{p}_{K^+K^-}(\mathbf{r}_{\rm cr},m_\phi)\mathbf{\Omega}^*_{K^-} \qquad (50)$$

and then averaging the quantity Δm over all possible values of the solid angle $\mathbf{\Omega}^*_{K^-}$ along which the K^- momentum $\overset{*}{\mathbf{p}}_{K^+K^-}$ in the ϕ rest frame is directed, we find

$$\overline{\Delta m}=-\frac{1}{2m_\phi}(\bar I_1+\bar I_2), \qquad (51)$$

where

$$\bar I_1=\frac{2I_{1+}\Delta_+}{a_+(\overline{\cos\theta^*_{K^-}})}+\frac{2I_{1-}\Delta_-}{a_-(\overline{\cos\theta^*_{K^-}})}, \qquad (52)$$

$$I_{1\pm}=\frac{p_\phi^2}{\overset{*}{p}^2_{K^+K^-}(\mathbf{r}_{\rm cr},m_\phi)}\left(\frac{1}{2}-\overline{\cos^2\theta^*_{K^-}}\right)$$
$$\mp\frac{p_\phi}{\overset{*}{p}_{K^+K^-}(\mathbf{r}_{\rm cr},m_\phi)}\overline{\cos\theta^*_{K^-}}, \qquad (53)$$

$$I_{2\pm} = \frac{\Delta_{\pm}^2}{\left[\bar{E}'^2_{K^\pm} - m^{*2}_{K^\pm}(\mathbf{r}_{\rm cr})\right] a^2_{\pm}(\overline{\cos\theta^*_{K^-}})},$$
$$I_{2+-} = \frac{\Delta_+\Delta_- \left[2\bar{E}'_{K^+}\bar{E}'_{K^-} + m^{*2}_{K^+}(\mathbf{r}_{\rm cr}) + m^{*2}_{K^-}(\mathbf{r}_{\rm cr}) - m^2_{\phi}\right]}{a_+(\overline{\cos\theta^*_{K^-}})a_-(\overline{\cos\theta^*_{K^-}})\left[\bar{E}'^2_{K^+} - m^{*2}_{K^+}(\mathbf{r}_{\rm cr})\right]\left[\bar{E}'^2_{K^-} - m^{*2}_{K^-}(\mathbf{r}_{\rm cr})\right]} \quad (57)$$

$$a_{\pm}(\overline{\cos\theta^*_{K^-}}) = 1 + \sqrt{\frac{\bar{E}'^2_{K^\pm} - m^2_K}{\bar{E}'^2_{K^\pm} - m^{*2}_{K^\pm}(\mathbf{r}_{\rm cr})}}, \quad (54)$$

$$\bar{E}'_{K^\pm} = \gamma_\phi\left(\overset{*}{E}_{K^\pm}(\mathbf{r}_{\rm cr}, m_\phi) \mp \overset{*}{p}_{K^+K^-}(\mathbf{r}_{\rm cr}, m_\phi) v_\phi \overline{\cos\theta^*_{K^-}}\right),$$

$$\overset{*}{E}_{K^\pm}(\mathbf{r}_{\rm cr}, m_\phi) = \sqrt{\overset{*2}{p}_{K^+K^-}(\mathbf{r}_{\rm cr}, m_\phi) + m^{*2}_{K^\pm}(\mathbf{r}_{\rm cr})}; \quad (55)$$

$$\bar{I}_2 = I_{2+} + I_{2-} + I_{2+-}, \quad (56)$$

see eqs. (57) *above*

and[20]

$$\overline{\cos\theta^*_{K^-}} = \begin{cases} 0, & \text{for } \kappa \le -1, \\ \frac{1+\kappa}{2}, & \text{for } -1 < \kappa \le 1, \end{cases}$$
$$\overline{\cos^2\theta^*_{K^-}} = \begin{cases} \frac{1}{3}, & \text{for } \kappa \le -1, \\ \frac{1+\kappa+\kappa^2}{3}, & \text{for } -1 < \kappa \le 1, \end{cases} \quad (58)$$

$$\kappa = \frac{m_K - \gamma_\phi \overset{*}{E}_{K^-}(\mathbf{r}_{\rm cr}, m_\phi)}{\gamma_\phi v_\phi \overset{*}{p}_{K^+K^-}(\mathbf{r}_{\rm cr}, m_\phi)}. \quad (59)$$

The kaon/antikaon momentum $\overset{*}{p}_{K^+K^-}$ in the phi rest frame is defined above by eq. (14). The effective kaon masses $m^*_{K^\pm}$, entering into eqs. (14), (45)-(59), include now in addition to the scalar hadronic potentials $U_{K^\pm}(\rho_N)$ also the Coulomb potential $V_{\rm C}(\mathbf{r})$ (cf. eq. (17))[21]

$$m^*_{K^\pm}(\mathbf{r}) = m_K + U_{K^\pm}(\rho_N(\mathbf{r})) \pm V_{\rm C}(\mathbf{r}). \quad (60)$$

In our calculations of the dikaon production cross-section on ^{63}Cu reported here this potential has been taken in the simple form corresponding to the interaction between the point kaon and the uniformly charged spherical core of charge Z [142]:

$$V_{\rm C}(\mathbf{r}) = \begin{cases} V_{\rm C}\left[\frac{3}{2} - \frac{1}{2}\left(\frac{r}{R_{\rm C}}\right)^2\right], & \text{for } r \le R_{\rm C}, \\ V_{\rm C}\frac{R_{\rm C}}{r}, & \text{for } r > R_{\rm C}, \end{cases} \quad (61)$$

[20] It should be mentioned that for $\kappa > 1$ the ϕ daughter K^--mesons produced at the point $\mathbf{r}_{\rm cr}$ cannot escape from the nucleus, since in this case their total energies are smaller than the free-kaon mass m_K (cf. eq. (27)).

[21] This is very well justified for the low-energy kaons of our interest, since their total energies inside the nuclear matter $\sqrt{\mathbf{p}'^2_{K^\pm} + (m_K + U_{K^\pm})^2} \pm V_{\rm C}$ can be sufficiently well approximated by the expression $\sqrt{\mathbf{p}'^2_{K^\pm} + (m_K + U_{K^\pm} \pm V_{\rm C})^2}$ in which the effective kaon masses incorporate the Coulomb potential.

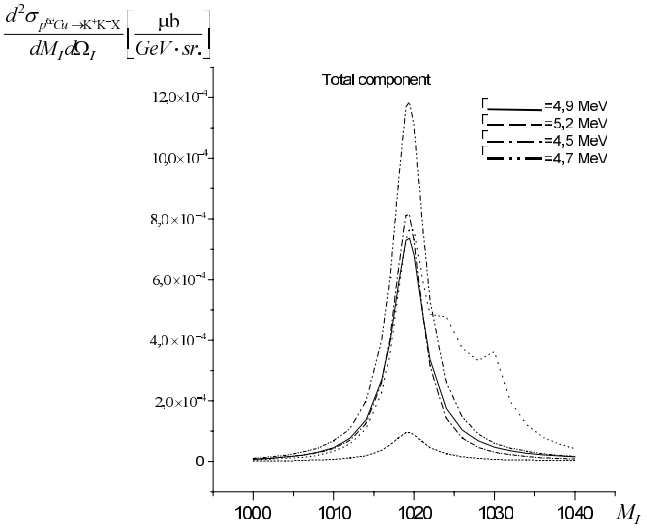

Fig. 13. Double differential invariant-mass cross-sections for the production of K^+K^- pairs from the decays of ϕ-mesons going forward in the nuclear lab frame both inside and outside of the ^{63}Cu target nuclei in the interaction of 2.4 GeV protons with these nuclei. The dotted line is the calculation at $p_{\rm cut} = 150$ MeV/c, $U_K(\rho_N) = 22(\rho_N/\rho_0)$ MeV, $U_{\bar{K}}(\rho_N) = -126(\rho_N/\rho_0)$ MeV, $\alpha_\rho = 0.18$, $\Gamma_{\rm coll} = 10(\rho_N/\rho_0)$ MeV employing the modification of the invariant mass of the K^+K^- pair due to the Coulomb and hadronic kaon potentials. The notation of the other curves is identical to that in fig. 10.

where $V_{\rm C} = 8.6$ MeV and $R_{\rm C} = 4.855$ fm.

Now, let us discuss the results of our full calculations for dikaon production in p^{63}Cu interactions in the framework of the model outlined above.

Figure 13 shows the resulting K^+K^- invariant-mass spectrum from $p + {}^{63}$Cu collisions at a beam energy of 2.4 GeV calculated by taking into account the above-introduced change of the invariant mass of the K^+K^- pair due to the Coulomb potential[22] and the hadronic kaon potentials using eqs. (25) and (43) (dotted line) in comparison to the previously performed calculations without employing any medium modifications for this mass (dashed, dot-dashed, double-dot–dashed and solid lines). Comparing dotted and solid lines corresponding to calculations with allowance for the influence of the same nuclear mean fields on the ϕ daughter kaons and rho meson

[22] It should be pointed out that the influence of this potential on the process of production of low-momentum kaon pairs inside the target nuclei under consideration as well as on the processes of production and propagation of such pairs outside these target nuclei was found to be negligible.

as well as with the use the same phi collisional width and momentum cutoff parameter $p_{\rm cut}$, we nicely see that the total dikaon invariant-mass distribution is broadened and shifted to higher invariant masses when the effect of the kaon potentials on the propagation of kaons and antikaons is taken into account[23] . Since the main contribution to the above-obtained modification of the K^+K^- invariant-mass spectrum comes from the hadronic kaon potentials, this means that the measurement of such a broad spectrum with an asymmetry to higher invariant masses as displayed in fig. 13 would give additional evidence for the renormalization of the kaon properties in nuclear matter. On the other hand, this spectrum cannot give any information about the modification of the ϕ spectral function at finite baryon density. Therefore, taking into account the above considerations, one may conclude that —even applying low-momentum cuts— it is impossible to observe the ϕ in-medium properties through the K^+K^- invariant-mass spectra from pA collisions.

3 Conclusions

In this paper we have investigated in a spectral function approach [111–115] the production and decay via the dikaon (dimuon) channel of ϕ-mesons in p^{12}C, p^{63}Cu reactions at 2.4 and 2.7 GeV beam energies. The production process included in our study is $pN \to pN\phi$. The momentum distributions of ϕ-mesons produced through this process which decay inside as well as outside of the ^{63}Cu target nucleus have been calculated at 2.4 and 2.7 GeV incident energies. It was shown that in the region of low ϕ momenta ($p_\phi \leq 100$ MeV/c) the contribution of in-medium decays is larger than the one from vacuum decays. A possible uncertainty of our calculations due to the poor knowledge of the elementary cross-sections for phi production from $p+p$ and $p+n$ interactions in the threshold energy region has been estimated. It was further demonstrated that the K^+K^- ($\mu^+\mu^-$) invariant-mass distribution consists of the two components which correspond to the ϕ decay outside and inside the target nucleus. The first (narrow) component has the free ϕ width, while the second (broad) component is distorted by the nuclear matter due to resonance-nucleon scattering and a possible in-medium modification of the kaons and ρ-meson at finite baryon density. The relative strength of the inside and outside components was analyzed in different scenarios for the phi width and momentum cut. Applying a cut of 100 MeV/c to the ϕ three-momentum, we have found a moderate broadening of the resulting dimuon invariant-mass distribution due to the total phi in-medium width from $p+{}^{12}$C collisions at 2.4 GeV beam energy compared to the situation in free space. Whereas in the case of $p+{}^{63}$Cu reactions at the same incident energy, we have obtained an observable enhancement of the width of the full $\mu^+\mu^-$ invariant-mass spectrum by a factor of about two. The enhancement is expected to be even larger for heavier target nuclei, since the relative weight of the dimuon inside component relative to the outside component, as showed by our calculations, increases with the atomic mass of the target nucleus. This gives in principle the opportunity to study the in-medium properties of the ϕ at finite baryon density experimentally by measuring the dilepton (dimuon or dielectron) yields for low-momentum cuts from the decays of phi mesons produced in the interaction of protons with medium and heavy target nuclei. Such measurements might be conducted at, for example, the accelerator SIS/GSI using proton beam in the HADES detector system.

On the other hand, because of the strong absorption of the K^- in nuclear matter, we found no measurable broadening of the resulting dikaon invariant-mass distributions due to the ϕ in-medium width both from $p+{}^{12}$C and from $p+{}^{63}$Cu interactions at 2.4 GeV when the respective cutoff for the phi three-momentum was applied. Contrary to the weak sensitivity of these distributions to the ϕ in-medium properties we also have found a rather strong impact of the kaon and antikaon final-state interactions (propagation in the Coulomb and hadronic kaon potentials) on the invariant-mass spectrum of the observed K^+K^- pairs. Due to these interactions (mainly due to the propagation in the hadronic kaon potentials) we have obtained for $p+{}^{63}$Cu collisions at 2.4 GeV a broadened spectrum with a distinct shift of spectral strength to higher invariant masses. This means that the measurement of such a broad K^+K^- spectrum with an asymmetry to higher invariant masses would give additional evidence for the modification of the kaon and antikaon properties in nuclear matter. On the other hand, this spectrum cannot give any information about the ϕ renormalization at finite baryon density. We, therefore, come to the conclusion that —even applying low-momentum cuts— it is not possible to observe the in-medium properties of the ϕ through the dikaon invariant-mass distributions from pA reactions.

The author is grateful to A.I. Berlev, F.F. Guber, A.S. Iljinov, Yu.T. Kiselev, A.B. Kurepin, A.I. Reshetin, M.G. Sapozhnikov, V.A. Sheinkman, E.A. Strokovsky for their interest in the work. It is also a pleasure to acknowledge the contribution of D.A. Biryukov to the preparation of the figures.

[23] It is worth mentioning that this is in line with the findings inferred in ref. [59] from studying the phi photoproduction off nuclei within the BUU transport model.

References

1. CERES Collaboration (G. Agakichiev *et al.*), Phys. Rev. Lett. **75**, 1272 (1995).
2. CERES Collaboration (G. Agakichiev *et al.*), Phys. Lett. B **422**, 405 (1998).
3. CERES Collaboration (G. Agakichiev *et al.*), Eur. Phys. J. C **4**, 231 (1998).
4. CERES Collaboration (G. Agakichiev *et al.*), Eur. Phys. J. C **4**, 249 (1998).
5. I. Ravinovich (for the CERES Collaboration), Nucl. Phys. A **638**, 159c (1998).
6. B. Lenkeit (for the CERES Collaboration), Nucl. Phys. A **661**, 23 (1999).

7. CERES Collaboration (Th. Ullrich *et al.*), Nucl. Phys. A **610**, 317c (1996).
8. CERES Collaboration (D. Adamova *et al.*), Phys. Rev. Lett. **91**, 042301 (2003).
9. HELIOS-1 Collaboration (T. Akesson *et al.*), Z. Phys. C **68**, 47 (1995).
10. M.A. Mazzoni (for the HELIOS-3 Collaboration), Nucl. Phys. A **566**, 95c (1994).
11. M. Masera (for the HELIOS-3 Collaboration), Nucl. Phys. A **590**, 93c (1995).
12. A. De Falco (for the NA38 Collaboration), Nucl. Phys. A **638**, 487c (1998).
13. R. Ferreira (for the NA38 Collaboration), Nucl. Phys. A **544**, 497c (1992).
14. NA50 Collaboration (E. Scomparin *et al.*), J. Phys. G **25**, 235 (1999).
15. P. Bordalo (for the NA50 Collaboration), Nucl. Phys. A **661**, 638 (1999).
16. D. Jouan (for the NA50 Collaboration), Nucl. Phys. A **681**, 157c (2001).
17. E-802 Collaboration (Y. Akiba *et al.*), Phys. Rev. Lett. **76**, 2021 (1996).
18. DLS Collaboration (R.J. Porter *et al.*), Phys. Rev. Lett. **79**, 1229 (1997).
19. DLS Collaboration (W.K. Wilson *et al.*), Phys. Rev. C **57**, 1865 (1998).
20. N. Herrmann (for the FOPI Collaboration), Nucl. Phys. A **610**, 49c (1996).
21. FOPI Collaboration (A. Mangiarotti *et al.*), Nucl. Phys. A **714**, 89 (2003).
22. KEK-PS-E325 Collaboration (H. En'yo *et al.*), Nucl. Phys. A **670**, 182c (2000).
23. KEK-PS-E325 Collaboration (K. Ozawa *et al.*), Phys. Rev. Lett. **86**, 5019 (2001).
24. KEK-PS-E325 Collaboration (K. Ozawa *et al.*), Nucl. Phys. A **698**, 535c (2002).
25. TAGX Collaboration (G.J. Lolos *et al.*), Phys. Rev. Lett. **80**, 241 (1998).
26. TAGX Collaboration (M.A. Kagarlis *et al.*), Phys. Rev. C **60**, 025203 (1999).
27. W. Cassing, E.L. Bratkovskaya, Phys. Rep. **308**, 65 (1999).
28. W. Cassing, W. Ehehalt, C.M. Ko, Phys. Lett. B **363**, 35 (1995).
29. W. Cassing, W. Ehehalt, I. Kralik, Phys. Lett. B **377**, 5 (1996).
30. G.Q. Li, C.M. Ko, G.E. Brown, Phys. Rev. Lett. **75**, 4007 (1995).
31. C.M. Ko, G.Q. Li, G.E. Brown, H. Sorge, Nucl. Phys. A **610**, 342c (1996).
32. G.Q. Li, C.M. Ko, G.E. Brown, H. Sorge, Nucl. Phys. A **611**, 539 (1996).
33. R. Rapp, G. Chanfray, J. Wambach, Phys. Rev. Lett. **76**, 368 (1996).
34. R. Rapp, G. Chanfray, J. Wambach, Nucl. Phys. A **617**, 472 (1997).
35. E.L. Bratkovskaya, W. Cassing, Nucl. Phys. A **619**, 413 (1997).
36. W. Cassing, E.L. Bratkovskaya, R. Rapp, J. Wambach, Phys. Rev. C **57**, 916 (1998).
37. E.L. Bratkovskaya, W. Cassing, R. Rapp, J. Wambach, Nucl. Phys. A **634**, 168 (1998).
38. W.S. Chung, G.Q. Li, C.M. Ko, Nucl. Phys. A **625**, 347 (1997).
39. W.S. Chung, C.M. Ko, G.Q. Li, Nucl. Phys. A **641**, 357 (1998).
40. Subrata Pal, C.M. Ko, Zi-wei Lin, Nucl. Phys. A **707**, 525 (2002).
41. Sourav Sarkar, Jan-e Alam, T. Hatsuda, Pramana **60**, 1073 (2002).
42. Sourav Sarkar, nucl-th/0201066.
43. P. Filip, E.E. Kolomeitsev, Phys. Rev. C **64**, 054905 (2001).
44. B. Kämpfer, O.P. Pavlenko, S. Zschocke, Eur. Phys. J. A **17**, 83 (2003).
45. Gy. Wolf, O.P. Pavlenko, B. Kämpfer, nucl-th/0306029.
46. Ye.S. Golubeva, A.S. Iljinov, L.A. Kondratyuk, Acta Phys. Pol. B **27**, 3241 (1996).
47. A. Sibirtsev, W. Cassing, Nucl. Phys. A **629**, 717 (1998).
48. A. Sibirtsev, V. Hejny, H. Ströher, W. Cassing, Phys. Lett. B **483**, 405 (2000).
49. Ye.S. Golubeva, L.A. Kondratyuk, M. Büscher, W. Cassing, V. Hejny, H. Ströher, Eur. Phys. J. A **11**, 237 (2001).
50. E.L. Bratkovskaya, W. Cassing, U. Mosel, Nucl. Phys. A **686**, 568 (2001).
51. W. Schön, H. Bokemeyer, W. Koenig, V. Metag, Acta Phys. Pol. B **27**, 2959 (1996).
52. Ye.S. Golubeva, L.A. Kondratyuk, W. Cassing, Nucl. Phys. A **625**, 832 (1997).
53. L.A. Kondratyuk, Ye.S. Golubeva, Phys. At. Nucl., **61**, N5, 865 (1998).
54. Th. Weidmann, E.L. Bratkovskaya, W. Cassing, U. Mosel, Phys. Rev. C **59**, 919 (1999).
55. M. Effenberger, E.L. Bratkovskaya, W. Cassing, U. Mosel, Phys. Rev. C **60**, 027601 (1999).
56. M. Effenberger, E.L. Bratkovskaya, U. Mosel, Phys. Rev. C **60**, 044614 (1999).
57. J.G. Messchendorp, A. Sibirtsev, W. Cassing, V. Metag, S. Schadmand, Eur. Phys. J. A **11**, 95 (2001).
58. E. Oset, M.J. Vicente Vacas, H. Toki, A. Ramos, Phys. Lett. B **508**, 237 (2001).
59. P. Muehlich, T. Falter, C. Greiner, J. Lehr, M. Post, U. Mosel, Phys. Rev. C **67**, 024605 (2003).
60. U. Mosel, nucl-th/0002020.
61. U. Mosel, nucl-th/0304080.
62. G.E. Brown, M. Rho, Phys. Rev. Lett. **66**, 2720 (1991).
63. T. Hatsuda, S.H. Lee, Phys. Rev. C **46**, R34 (1992).
64. T. Renk, R.A. Schneider, W. Weise, Nucl. Phys. A **699**, 1c (2002).
65. G. Paic, Nucl. Phys. A **699**, 114c (2002).
66. W. Weise, Nucl. Phys. A **690**, 98c (2001).
67. U. Mosel, nucl-th/9811065.
68. M. Herrmann, B.L. Friman, W. Norenberg, Nucl. Phys. A **560**, 411 (1993).
69. M. Urban, M. Buballa, R. Rapp, J. Wambach, Nucl. Phys. A **673**, 357 (2000).
70. R. Rapp, J. Wambach, Adv. Nucl. Phys. **25**, 1 (2000).
71. D. Cabrera, E. Oset, M.J. Vicente Vacas, Nucl. Phys. A **705**, 90 (2002).
72. H. Shiomi, T. Hatsuda, Phys. Lett. B **334**, 281 (1994).
73. H. Kuwabara, T. Hatsuda, Prog. Theor. Phys. **94**, 1163 (1995).
74. F. Klingl, T. Waas, W. Weise, Phys. Lett. B **431**, 254 (1998).
75. E. Oset, A. Ramos, Nucl. Phys. A **679**, 616 (2001).

76. D. Cabrera, M.J. Vicente Vacas, Phys. Rev. C **67**, 045203 (2003).
77. L.A. Kondratyuk, A. Sibirtsev, W. Cassing, Ye.S. Golubeva, M. Effenberger, Phys. Rev. C **58**, 1078 (1998).
78. B. Friman, M. Lutz, G. Wolf, nucl-th/9811040.
79. B. Friman, M. Lutz, G. Wolf, nucl-th/0003012.
80. M. Post, U. Mosel, Nucl. Phys. A **699**, 169c (2002).
81. G. Chanfray, Nucl. Phys. A **721**, 76 (2003).
82. S. Zschocke, O.P. Pavlenko, B. Kämpfer, Eur. Phys. J. A **15**, 529 (2002).
83. A.I. Titov, B. Kämpfer, V.V. Shklyar, Phys. Rev. C **59**, 999 (1999).
84. A.I. Titov, B. Kämpfer, B.L. Reznik, Eur. Phys. J. A **7**, 543 (2000).
85. A.I. Titov, B. Kämpfer, B.L. Reznik, nucl-th/0102032.
86. F. Balestra *et al.*, Phys. Rev. Lett. **81**, 4572 (1998).
87. P. Koch, B. Müller, J. Rafelski, Phys. Rep. **142**, 167 (1986).
88. A. Shor, Phys. Rev. Lett. **54**, 1122 (1985).
89. D. Lissauer, E. Shuryak, Phys. Lett. B **253**, 15 (1991).
90. F. Klingl, N. Kaiser, W. Weise, Nucl. Phys. A **624**, 527 (1997).
91. K. Haglin, Nucl. Phys. A **584**, 719 (1995).
92. W. Smith, K. Haglin, Phys. Rev. C **57**, 1449 (1998).
93. A. Bhattacharyya, S.K. Ghosh, S.C. Phatak, S. Raha, Phys. Rev. C **55**, 1463 (1997).
94. H.W. Barz, M. Zetenyi, Gy. Wolf, B. Kämpfer, Nucl. Phys. A **705**, 223 (2002).
95. C.M. Ko, B.H. Sa, Phys. Lett. B **258**, 6 (1991).
96. NA49 Collaboration (S.V. Afanasiev *et al.*), Phys. Lett. B **491**, 59 (2000).
97. NA50 Collaboration (M.C. Abreu *et al.*), J. Phys. G **27**, 405 (2001).
98. STAR Collaboration (C. Adler *et al.*), Phys. Rev. C **65**, 041901(R) (2002).
99. DISTO Collaboration (F. Balestra *et al.*), Phys. Rev. C **63**, 024004 (2001).
100. CLAS Collaboration (E. Anciant *et al.*), Phys. Rev. Lett. **85**, 4682 (2000).
101. SAPHIR Collaboration (J. Barth *et al.*), Eur. Phys. J. A **17**, 269 (2003).
102. HADES Collaboration (J. Friese), Prog. Part. Nucl. Phys. **42**, 235 (1999).
103. B. Kämpfer, R. Kotte, C. Hartnack, J. Aichelin, J. Phys. G **28**, 2035 (2002).
104. V.Yu. Alexakhin *et al.*, NIS Project, JINR, Dubna.
105. M. Büscher *et al.*, ANKE COSY proposals #21 (1996), #104 (2001).
106. T. Nakano *et al.*, Nucl. Phys. A **684**, 71c (2001).
107. H.W. Barz, M. Zetenyi, nucl-th/0310045.
108. D. Cabrera, L. Roca, E. Oset, H. Toki, M.J. Vicente Vacas Nucl. Phys. A **733**, 130 (2004).
109. V.K. Magas, L. Roca, E. Oset, nucl-th/0403067.
110. E.Ya. Paryev, preprint INR-1119/2004, Moscow (April 2004).
111. S.V. Efremov, E.Ya. Paryev, Eur. Phys. J. A **1**, 99 (1998).
112. E.Ya. Paryev, Eur. Phys. J. A **5**, 307 (1999).
113. E.Ya. Paryev, Eur. Phys. J. A **7**, 127 (2000).
114. E.Ya. Paryev, Eur. Phys. J. A **9**, 521 (2000).
115. E.Ya. Paryev, Eur. Phys. J. A **17**, 145 (2003).
116. K.G. Boreskov, J.H. Koch, L.A. Kondratyuk, M.I. Krivoruchenko, Yad. Fiz. **59**, 1908 (1996).
117. Particle Data Group (D.E. Groom *et al.*), Eur. Phys. J. C **15**, 1 (2000).
118. D.M. Manley, E.M. Saleski, Phys. Rev. D **45**, 4002 (1992).
119. A. Sibirtsev, Ch. Elster, J. Haidenbauer, J. Speth, nucl-th/0104011.
120. C. Gobbi, C. Dover, A. Gal, Phys. Rev. C **50**, 1594 (1994).
121. A. Ramos, E. Oset, Nucl. Phys. A **671**, 481 (2000).
122. J. Schaffner-Bielich, V. Koch, M. Effenberger, Nucl. Phys. A **669**, 153 (2000).
123. M. Lutz, Phys. Lett. B **426**, 12 (1998).
124. A. Cieply, E. Friedman, A. Gal, J. Mares, Nucl. Phys. A **696**, 173 (2001).
125. A. Ramos, S. Hirenzaki, S.S. Kamalov, T.T.S. Kuo, Y. Okumura, E. Oset, A. Polls, H. Toki, L. Tolós, nucl-th/0101031.
126. L. Tolós, A. Ramos, A. Polls, T.T.S. Kuo, Nucl. Phys. A **690**, 547 (2001).
127. L. Tolós, A. Ramos, A. Polls, Phys. Rev. C **65**, 054907 (2002).
128. S. Leupold, W. Peters, U. Mosel, Nucl. Phys. A **628**, 311 (1998).
129. S. Mallik, A. Nyffeler, Phys. Rev. C **63**, 065204, (2001).
130. W. Peters, M. Post, H. Lenske, S. Leupold, U. Mosel, Nucl. Phys. A **632**, 109 (1998).
131. V.L. Eletsky, B.L. Ioffe, Phys. Rev. Lett. **78**, 1010 (1997).
132. V.L. Eletsky, B.L. Ioffe, J.I. Kapusta, Eur. Phys. J. A **3**, 381 (1998).
133. V.L. Eletsky, B.L. Ioffe, J.I. Kapusta, Nucl. Phys. A **661**, 514 (1999).
134. V.L. Eletsky, J.I. Kapusta, Phys. Rev. C **59**, 2757 (1999).
135. V.L. Eletsky, M. Belkacem, P.J. Ellis, J.I. Kapusta, Phys. Rev. C **64**, 035202 (2001).
136. B.K. Jain, B. Kundu, Phys. Rev. C **53**, 1917 (1996).
137. B. Kundu, B.K. Jain, Pramana **56**, 723 (2001).
138. A. Sibirtsev, W. Cassing, U. Mosel, Z. Phys. A **358**, 357 (1997).
139. Y. Nara, A. Ohnishi, T. Harada, A. Engel, Nucl. Phys. A **614**, 433 (1997).
140. C. Ciofi degli Atti, S. Simula, Phys. Rev. C **53**, 1689 (1996).
141. A. Ramos, A. Polls, W.H. Dickhoff, Nucl. Phys. A **503**, 1 (1989).
142. A. Bohr, B.R. Mottelson, *Nuclear Structure*, Vol. **1** (W.A. Benjamin Inc., New York, Amsterdam, 1969).